GEOCHEMISTRY OF MOLYBDENUM IN THE AQUIA AQUIFER, MARYLAND, USA

by

TERESA IAFELICE VALLE

Presented to the Faculty of the Graduate School of

The University of Texas at Arlington in Partial Fulfillment

of the Requirements

for the Degree of

MASTER OF SCIENCE IN GEOLOGY

THE UNIVERSITY OF TEXAS AT ARLINGTON

December 2009

DEDICATION

In memory of Daisy, beloved companion

ACKNOWLEDGEMENTS

Writing a thesis is a difficult task and I could not have finished this project without the support of many people along the way. I would like to express my gratitude to Dr. Harry Rowe, my thesis supervisor, for all his candid editorial comments and valuable knowledge. I would also like to thank my thesis committee members: Dr. John Wickham and Dr. John Holbrook for their encouragement. I would like to thank the sampling crew that accompanied me to Maryland, Heeral Dave and Stephanie Willis. Stephanie Willis deserves special thanks for her patients and helpful insight in the operation of the ICP-MS and her eagerness to answer any of my questions. In closing I would like to thank all my friends and family, for their unconditional love and support. They were always there for me when I was stressed out and needed someone to complain to without their undying support this thesis would not have been completed.

November 13, 2009

ABSTRACT

GEOCHEMISTRY OF MOLYBDENUM IN THE

AQUIA AQUIFER, MARYLAND, USA

Teresa Iafelice Valle, M.S.

The University of Texas at Arlington, 2009

Supervising Professor: Harold Rowe

The present study contributes to the understanding of controls on and behavior of molybdenum (Mo) in an aquifer, and its potential as an indicator of changing redox conditions along the groundwater flowpath. The central hypothesis of the present work is that the hydrogeochemical evolution along two separate groundwater flowpaths of the Aquia Aquifer, Maryland, USA, one each on the Eastern and Western Shore of Chesapeake Bay, consists of chemical weathering and oxidation-reduction reactions that dictate the degree of Mo mobilization, as well as mineral co-precipitation/re-adsorption reactions that dictate the degree of Mo immobilization (i.e., scavenging). This hypothesis is evaluated by defining the relationship between the concentration of Mo, the concentration and speciation of dissolved constituents (e.g., Fe, S^{2-}, Mn, and N), and the bulk hydrochemical parameters (e.g., alkalinity, pH, DO, and Eh) along the groundwater flowpaths. It is anticipated that the integration of these hydrogeochemical results will demonstrate and further explain 1) the differences in the groundwater evolution between the two Aquia flowpaths, 2) the underlying differences between the Aquia Aquifer and other aquifers, and most importantly, 3) the unique utility of Mo as a groundwater tracer. In order to accomplish these objectives, a series of groundwater samples

were collected along the inferred Eastern and Western Shore flowpaths of the Aquia Aquifer. Results of the comparison in groundwater evolution between the two Aquia flowpaths reveal that the redox boundary for both flowpaths correlates with the cation-exchange reaction identified by the change in water chemistry. This is evident near the recharge zone, where waters are identified as Ca-Mg-HCO_3^- type and at locations near the redox boundary (~52.5 – 57 km), where water chemistry evolves to Na-HCO_3^- type. The present study concludes that Mo can be used as an indicator of changing redox conditions. Molybdenum shows an overall increase in concentration along both flowpaths as a result of reducing conditions. Results from the Eastern Shore flowpath indicate that high concentrations of Mo (1.493 μmol kg^{-1}, at 55 km) are the results of pH-induced desorption/dissolution and microbial dissimilatory processes. At distances greater than 80 km from the recharge zone, Mo decreases in concentration (1.183 – 0.354 μmol kg^{-1}) due to co-precipitation/re-adsorption processes associated with the development of crystallized Fe^{2+} sulfides that form coatings on aquifer mineral surfaces (i.e., pyrite, Chapelle and Knobel, 1983). Results from the Western Shore flowpath reveal an increase in Mo concentration (0.085 – 0.332 μmol kg^{-1}) at a distance of ~44 km from the recharge zone. This indicates that the release of Mo into solution is the direct result of initial Fe^{3+} reduction and respiratory microbial consortia present within the aquifer. At distances greater than ~55 km, Mo increases from 0.186 to 0.409 μmol kg^{-1}, which correlates with the complete reduction of iron. The highest concentration of Mo (0.461 μmol kg^{-1}) along the Western Shore flowpath coincides with strongly reducing waters, identified at distances greater than ~70 km along flowpath (pH > 9.0, Eh < -120).

TABLE OF CONTENTS

LIST OF ILLUSTRATIONS

Figure Page

LIST OF TABLES

CHAPTER 1
INTRODUCTION

1.1 Reduction-Oxidation Processes

Redox processes are an important control on the chemical evolution of an aquifer. A redox boundary marks the change in speciation of a redox-sensitive element and the associated change in its mobility along the groundwater flowpath of an aquifer system (Schlieker et al., 2001; Smedley and Edmunds, 2002). A geochemical analysis of groundwaters, and specifically, the concentrations of key redox-sensitive elements along a groundwater flowpath, helps assess the dominant controls on aquifer redox processes and their spatial and temporal variability. Demarcation of redox boundaries is important for a general understanding of groundwater evolution, but more practically, for groundwater management, as the location of a redox boundary may control the attenuation of contaminants such as nitrate, provided that electron donors are available, for example, for denitrification to occur (Champ and Gulens, 1978; Schlieker et al., 2001; Smedley and Edmunds, 2002).

Champ and Gulens (1978) consider redox and microorganism processes in the groundwater flow system of Perch Lake Basin at Chalk River, Ontario, Canada, from a qualitative point of view and have concentrated on describing the overall changes in the confined aquifer. In the recharge area groundwater initially contains dissolved oxidized species (O_2, NO_3^-, SO_4^{2-}, and CO_2) and also dissolved organic carbon (DOC). After entering the confined portion of the aquifer, the groundwater is then closed to the input of further oxidants or oxidized species. In the confined system it is thought that DOC and microbial activity facilitate the reduction of various oxidized species present in the groundwater. Carbon (both inorganic and organic) was found to be available, as well as elements (H, O, N, P, and S), minerals (K, Na, Mg, Ca, and Fe), and trace metals (Mn, Zn, Cu, Co, and Mo) which provide the necessary

nutrients required for biosynthetic activities of microorganisms (Champ and Gulens, 1978). Also available, were electron donors (DOC, H_2S, NH_3, Fe^{2+}) and electron acceptors (DO, NO_3^-, Fe^{3+}, Mn^{4+}, SO_4^{2-}, CO_2), which are required for energy generation of microorganisms (Champ and Gulens, 1978). Champ and Gulens (1978) conclude that after entering into a confined aquifer the oxidized species will reduce in the sequence of O_2, NO_3^-, Mn(IV), Fe^{3+}, SO_4^{2-}, HCO_3^-, and N_2 (McBride, 1994). As reduction continues, the measured potential of the groundwater, Eh, will become less positive due to the lower free energy change of each subsequent reaction. Equilibrium is needed for the redox potential to accurately measure the redox couple (Kehew, 2001). In many natural waters, disequilibrium is common because of the widespread presence of ongoing microbial processes; therefore, Eh values cannot be used as a quantitative indicator of redox processes (Kehew, 2001). For this reason, Champ and Gulens most likely used Eh measurements as relative values to generally characterize the changes along the groundwater flowpath. Following Champ and Gulens research, three successive biochemical zones were discovered by Golwer and others (1976), consequently providing support for the identification of redox zones on the basis of both biochemical and microbiological data.

Microorganisms that inhabit groundwater systems sustain their life functions with reduction/oxidation processes. Microorganisms effect many geochemical changes in groundwater. A microorganism need both electron donors (C, Fe^{2+}, Mn^{2+}, H_2S) and electron acceptors (O_2, NO_3^-, Mn^{4+}, Fe^{3+}, SO_4^{2-}, CO_2) to maintain the work to accomplish all of its life functions, including cellular maintenance, genetic expression, protein synthesis, growth, and reproduction (Penny and Lee, 2003). The net effect of these processes is to segregate aquifers into zones dominated by certain electron-accepting processes (Lovley et al., 1994). Lovley and Chapelle (1995) indicate that nonbiological models do not accurately describe or predict important geochemical processes; this is due to the fact that redox reactions do not take place spontaneously but require microorganisms to catalyze them.

1.2 Background Information on Molybdenum

Molybdenum is a redox-sensitive metal that occurs in low, but measureable abundances in aquifers. Molybdenum is the lightest metal in the periodic table (Z = 42; AW = 95.94 g/mol) whose metal-oxygen bond is characterized as being easily formed and/or broken (McEwan et al., 2001). Because the breakage of the Mo-O bond in the Mo-oxyanion complex ($(MoO_4)^{2-}$) requires very little energy, Mo is said to possess a high reducing potential, and under certain conditions it may be a useful indicator of reducing environments. Furthermore, Mo is the only element in the second row of transition metals that is an important nutrient for animal and plant life; however, excessive amounts of Mo intake/uptake are known to be toxic to some animals (Kaback and Runnels, 1979).

A considerable amount of research has been conducted on the geochemistry of Mo in marine environments (Crusius et al., 1996; Crusius and Thomson, 2000; Vorlicek et al., 2004, Algeo and Lyons, 2006; Algeo et al., 2007; Tribovillard et al, 2006, Tribovillard et al., 2008; Algeo and Maynard, 2008), but much less work has been undertaken to explain the geochemistry of Mo and how it may correlate with redox conditions within a confined aquifer. In oxic waters, the oxidized form of Mo^{6+} (Mo(VI)) is thought to be molybdate (MoO_4^{2-}) (Helz et al., 1996; Hodge et al., 1996). Soluble MoO_4^{2-} is found in waters that have a high Eh (redox potential) and low pH (6.5-7.5). Eh-pH relationships and the amount of iron oxides (e.g., co-precipitation/re-adsorption and desorption/dissolution processes), are known to control the mobility of Mo (Barakso and Bradshaw, 1971).

In suboxic environments Mo(VI) will reduce to Mo(IV) (Crusius et al., 1996). Molybdenum (IV) is released into pore water as a result of reductive dissolution of Mn and Fe in suboxic waters (Schlieker et al., 2001). Smedley and Edmunds (2002) study of the East Midlands Triassic Sandstone Aquifer, UK, reveal that Mo increases along flow gradient under high pH (>8) and low Eh (redox-potential decrease of some 300 mV) conditions. This is most likely the result of the lack of SO_4^{2-} reduction in the main confined aquifer (i.e., suboxic

environment). Sulfide generated *via* sulfate reduction and sufficient amounts of dissolved Fe^{2+} combine to form iron sulfides in the sediment, which may initially maintain H_2S at very low concentrations, thereby buffering the pH at a value that inhibits Mo mobility (Crusius et al., 1996).

Schlieker and others (2001) investigated the influence of the major redox processes on the mobility of the trace elements Cu, Zn, As, Mo, Ba, La, and Ce along a bank infiltration system of a sandy sediment anoxic Pleistocene aquifer from the Ruhr Valley (Western Germany). Their results show that the geochemistry of the trace elements involved can be explained to a large extent by major redox reactions involving manganese, iron, and sulfate. Specifically, their work supports reductive dissolution of Mn and Fe oxy-hydroxides as a major cause of Mo mobilization and its release to pore water in an aquifer system. Furthermore, they hypothesize that Mo may exist as either Mo(IV) within iron and manganese (hydr)oxides, or Mo(VI) (i.e., MoO_4^{2-}) adsorbed as an oxyanion to their solid-phase surfaces.

1.3 Hypothesis

The central hypothesis of the present work is that changes in the occurrence and extent of dissolved Mo occurring along groundwater flowpaths in the Aquia Aquifer of both the Eastern and Western Shores of Chesapeake Bay are the result of chemical weathering and oxidation-reduction reactions, as well as co-precipitation/re-adsorption reactions. Defining down-gradient concentrations of Mo and relating them to the hydrogeochemical changes occurring along flowpath will contribute 1) a stronger understanding of Mo affinity, mobility, and fate within an important aquifer system, 2) a more complete consideration of how different portions of one aquifer or how various aquifers differ in their hydrogeochemical evolution along flowpath, and 3) an enhanced perspective on how Mo is used to understand hydrogeochemical processes.

CHAPTER 2
HYDROGEOLOGIC SETTING

The Aquia Aquifer, located in the southeast region of Maryland (MD) in the Coastal Plain aquifer system (Figure 3), is a hydrostratigraphic unit defined within the broader Aquia Formation. It is described as a confined unit in an unconsolidated hydrogeologic formation (Chapelle and Knobel, 1983; Knobel et al., 1987). In general the aquifer is estimated to be 30 to 45 meters thick (Klohe & Kay, 2007). The Aquia formation consists predominantly of quartz sand (50 to 75%), shell debris, and a considerable amount of glauconite (20 to 40%), which gives the sediment its characteristic greenish color (Chapelle and Knobel,1983; Aeschbach-Hertig et al., 2002). The mineralogy of the unconsolidated sediments found in the Aquia is characteristic of marine, marginal marine and nonmarine depositional conditions. Sediments deposited under nonmarine to marginal marine conditions are commonly pyrite, lignite, and feldspar (Chapelle and Knobel, 1983; Knobel et al., 1987). Sediments deposited under marine conditions consist of authigenic minerals such as glauconite and shell material (Chapelle and Knobel, 1983; Knobel et al., 1987). Based on the mineral composition and location of these sediments, the Paleocene Aquia formation of Maryland has been interpreted as having been deposited in a regressive marine environment (Dai et al., 2006). The Eastern Shore flowpath is located on the Delmarva Peninsula, east of Chesapeake Bay. The hydrostratigraphic section compiled by Bachman and others (2002) illustrates that the Aquia is overlain by a surficial aquifer known as the Pensauken Formation (i.e., Columbia Aquifer, Figure 1). The Aquia and the Columbia Aquifers are considered to be hydraulically connected. The base of the Aquia Formation is composed of silt-clay material and therefore is considered to be very impermeable, making the Aquia and the Hornerstown Aquifer, which underlies the Aquia, to be less hydraulically connected (Bachman et al., 2002).

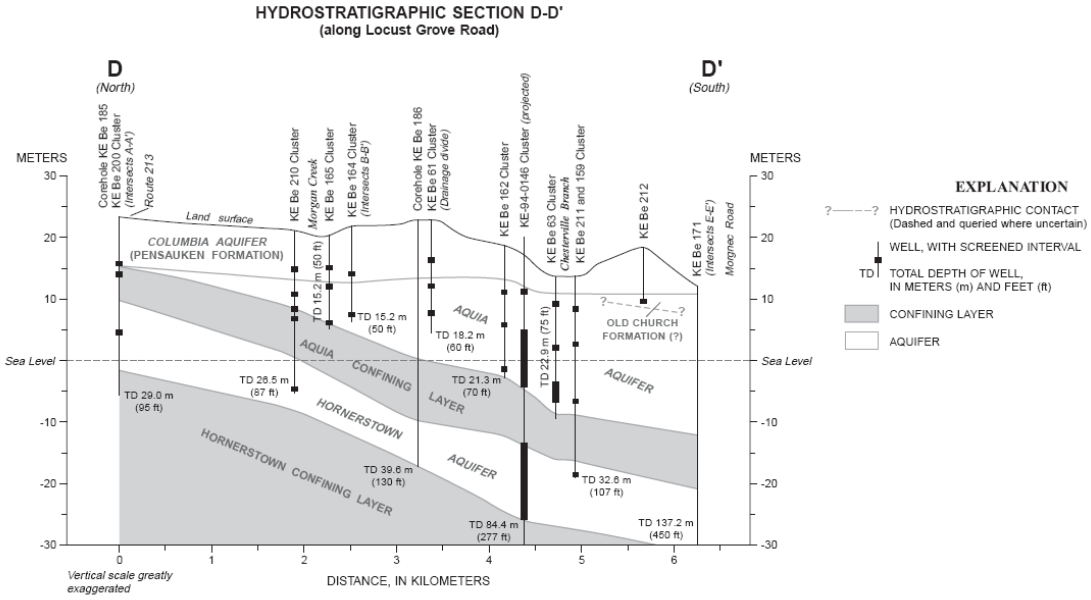

Figure 1: Hydrogeologic cross-section taken from Bachman et al., (2002), illustrating the hydrostratigraphic sequence on the eastern side of the Chesapeake Bay in Kent County, Maryland.

On the western shore of Chesapeake Bay, the Aquia Aquifer is underlain by the Severn Formation and overlain by the Marlboro Clay (Chapelle and Knobel, 1983; Aeschbach-Hertig et al., 2002; Figure 2). The Aquia Aquifer, as a whole, dips to the southeast and terminates in a facies change to more clay-rich impermeable sediment roughly 90 km from the outcrop area (Chapelle and Knobel, 1983; Aeschbach-Hertig et al., 2002). The Aquia Aquifer is a groundwater source for many residents in the region. According to the Maryland Department of Natural Resources (Andreasen, 2002), groundwater pumped from individual wells tapping the Aquia Aquifer supplied approximately 1.6 million gallons per day (Mgal/d) to an estimated 26,400 residents in 2000. An additional 0.18 Mgal/d was withdrawn from the Aquia Aquifer for mobile home parks and irrigation.

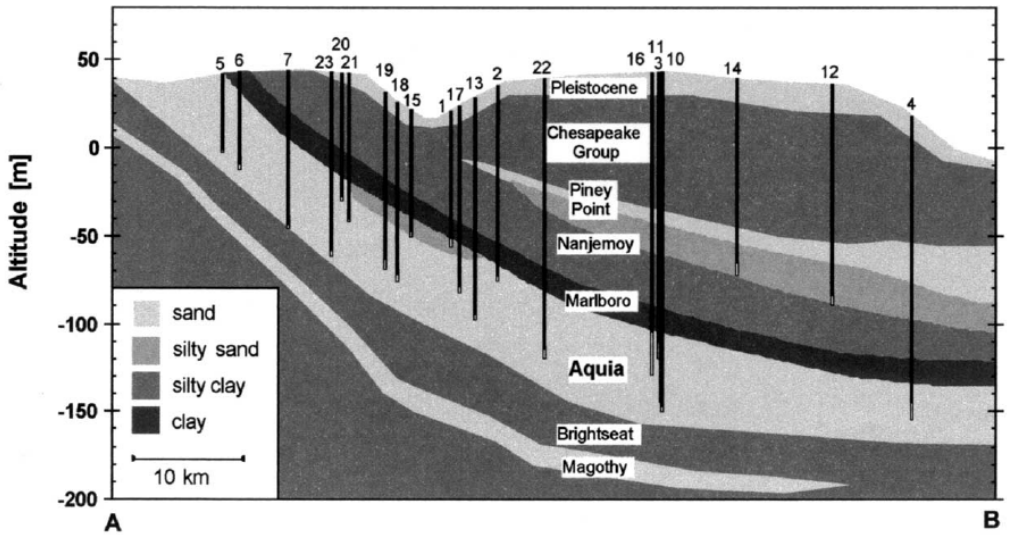

Figure 2: Hydrogeologic cross-section taken from Aeschbach-Hertig et al. (2002), illustrating the hydrostratigraphic sequence on the western side of the Chesapeake Bay in Calvert County, Maryland.

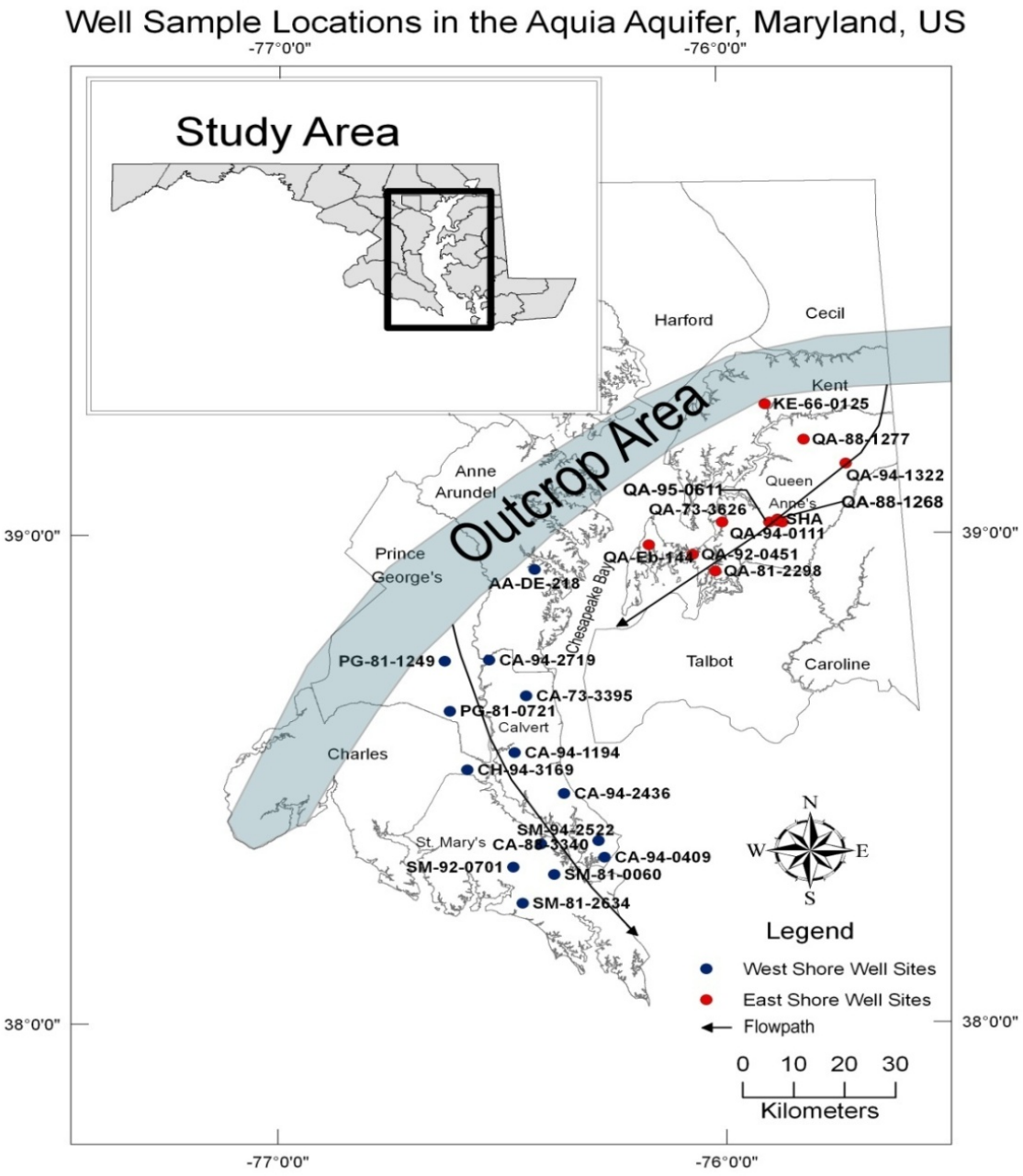

Figure 3: Map of the area studied, outcrop (recharge zone), and the sampled wells on the Eastern and Western Shore flowpaths.

To demonstrate general redox patterns and changes in chemistry along flowpath, the results of the study are plotted as a function of distance from the outcrop/recharge zone along hypothesized flow lines (Figure 3). Flow lines and distances were roughly estimated on the

basis of the pre-pumping potentiometric surface (Chapelle and Drummond, 1983). The first inferred flowpath is on the eastern shore of Chesapeake Bay, where the Aquia confining layers subcrop (within 5 meters of the land surface; Bachman et al., 2002) to the north where groundwater is recharged (e.g., northern Kent County, and southern Harford and Cecil County, Maryland), and subsequently flows southwest, discharging into the Chesapeake Bay in the vicinity of Kent Island, Queen Anne's County, Maryland (Haque and Johannesson, 2007; Haque et al., 2008). The second inferred flowpath is on the western shore of Chesapeake Bay, where groundwater is recharged to the north between Washington D.C. and Annapolis (e.g., northern Arundel, Prince Georges and Charles Counties) and flows southeast toward Chesapeake Bay (Aeschbach-Hertig et al., 2002; Klohe and Kay, 2007). The two flowpaths are referred to as the "Eastern Shore flowpath" and the "Western Shore flowpath", respectively, throughout the remainder of this paper.

CHAPTER 3
REGIONAL HYDROGEOCHEMISTRY: PREVIOUS WORK

Studies on the quality and quantity of Aquia groundwater have been conducted by several research groups (Chapelle and Knobel, 1983; Knobel et al., 1987; Andreasen, 2002; Gerhart and Cleaves, 2005). Extensive research describing the spatial difference in mineralogical composition and its effect on the chemical character of the groundwater of the Aquia is reported by Chapelle and Knobel (1983) and Knobel and others (1987). These studies found the dominant chemical processes acting in the aquifer are silicate hydrolysis, cation exchange, and reaction of groundwater with pyrite and lignite. Based on their findings, the aquifer is divided into three regions possessing unique chemical processes that control the overall character of the groundwater (Chapelle and Knobel, 1983).

Knobel and others (1987) described the geochemical processes that control the character of groundwater in the Aquia by implementing the findings of Chapelle and Knobel (1983). They concluded that in Region 1 (~0–40km, Figure 3), Ca^{2+} and Mg^{2+} concentrations increase, which is thought to be the result of rapid dissolution of high-magnesium calcite shell material in the presence of CO_2. Groundwater in Region 1 is known to be Ca-Mg bicarbonate in type. Dissolved oxygen concentrations are relatively high in Region 1. Shell material found in Region 1 is composed of magnesium calcite and aragonite and is commonly associated with secondary calcite cementation near the recharge area (Knobel et al., 1987). Down-gradient, the incongruent dissolution of glauconite is an important chemical process that consumes dissolved oxygen and releases SiO_2 into the groundwater. Microbial activity also consumes oxygen (Hunter et al., 1998; Vanbroekhoven et al., 2007), and has been reported to be present in the Aquia Aquifer (Chapelle, 2000; Pearcy, 2009).

In Region 2 (~40-70km, Figure 3), Knobel and others (1987) identified bicarbonate concentration as being several times higher than those that could be generated by reactions involving dissolved CO_2 gas in the recharge zone (Region 1). They found that stable carbon isotopes used in conjunction with major-ion water chemistry are useful for identifying the sources of HCO_3^- in the groundwater. The process of ion-exchange reactions, defined as the exchange of Ca^{2+} and Mg^{2+} for Na^+ facilitated by the surface of glauconite as the exchange medium, accounts for the down-gradient generation of sodium bicarbonate. The bicarbonate becomes enriched with the heavier isotope (^{13}C) with distance along the flowpath. In Region 2, the increase of HCO_3^- concentrations is more pronounced.

Knobel and others (1987) concluded that Region 3 (~70–90km, Figure 3) is characterized by an increase in Na^+ and HCO_3^- concentrations. The increase in concentrations of sodium coincides with the availability of Na^+ on glauconite. Bicarbonate concentrations increase due to the dissolution of these minerals and waters are considered to be Na-HCO_3-type.

Dai and Samper (2006) created a geochemical model of the Aquia Aquifer. The model revealed that the dominant geochemical processes acting in the aquifer are cation exchange and calcite dissolution. Based on an inverse model of water flow and multicomponent reactive transport in the Aquia, a later paper by Dai and others (2006) supports the idea that the dominant reaction controlling the geochemical evolution of the aquifer is cation exchange. This inverse model also focused on the displacement of seawater by freshwater in the Aquia. Based on the findings, estimated values of initial concentrations indicate that the initial water in the Aquia was not pure seawater but a mixture of seawater and freshwater. The model also addressed the possibility of the Aquia Aquifer leaking waters through the confining layer above the Aquia formation. Dai and others (2006) provided evidence suggesting that approximately 96% of recharge water leaks through to the confining layers above, and only a small portion of the recharge water (4%) continues down-gradient to the discharge zone.

Aeschbach-Hertig and colleagues conducted the most recent study on the age of the Aquia groundwaters in 2002. Dissolved concentrations of atmospheric noble gases were used to derive a mean annual ground temperature during the time of infiltration of the Aquia. Using earlier studies by Purdy and others (1992) as a foundation, scientists were able to use isotopes from the groundwater to estimate the age of the confined region of the Aquia Aquifer. The low ^{14}C activities of groundwater in the confined part of the aquifer of southeastern Maryland suggest that most infiltration occurred at least 100,000 years ago (Aeschbach-Hertig et al., 2002). Consequently, no anthropogenic pollutants were present at the time of infiltration, and all processes that are inferred to have occurred in the aquifer are the result of mineralogical composition, water-mineral interaction, and microbial activity (Chapelle and Knobel, 1983).

Table 1: An organized list of works by which flowpath was the focus of their study on the Aquia Aquifer.

Eastern Shore Flowpath	Western Shore Flowpath
Chapelle and Knobel, 1983	Chapelle and Knobel, 1983
Bachman et al., 2002	Chapelle and Knobel, 1985
Haque et al., 2007	Chapelle, 1983
	Knobel et al., 1987
	Purdy et al., 1992
	Appelo, 1994
	Purdy et al., 1996
	Andreasen, 2002
	Aeschbach-Hertig et al., 2002
	Dai and Samper, 2006
	Dai et al., 2006
	Klohe and Kay, 2007

3.1 Dataset Background for Current Project

The water samples from the Eastern Shore flowpath were collected by Shama Haque and Dr. Karen Johannesson for groundwater arsenic (As) study (Haque, 2007). Samples from the Western Shore flowpath were obtained in June 2007 by a group of hydrogeochemistry students, including the author, to form a more comprehensive dataset for the present study. Figure 3 shows the location of the sample well sites along the Western and Eastern Shore flowpaths of the Aquia Aquifer, the outcrop (recharge) areas, and the direction of flow within the aquifer. Table 2 lists the hydrogeochemical data from the Eastern Shore flowpath, and one sample from the Western Shore flowpath (AA DE 218) that was taken during sampling in 2006. Table 3 lists the concentrations and speciation for dissolved Fe, S, Mn, N, and Si calculated for the results listed in Table 2. The concentration/speciation data include: dissolved Fe species (II and III), sulfide (S^{2}), total dissolved Mn, dissolved N species (NH_4^+ and NO_3^-), and total Si. Molybdenum concentrations from the Eastern Shore flowpath are documented in Table 4. A table of these hydrogeochemical (Table 5) and the concentration/speciation data for Western Shore samples (Table 6) are included. Molybdenum concentrations from the Western Shore flowpath of the Aquia are listed in Table 7.

CHAPTER 4
MATERIALS AND METHODS

4.1 Field Approach

High-Density Poly-Ethylene bottles (HDPE), Teflon® tubing, Low-Density Poly-Ethylene (LDPE) cubitainers®, and lab-ware were cleaned using trace element clean (i.e., “trace clean”) procedures, accomplished by an acid wash and a triple rinse with deionized water (Johannesson et al., 2004).The cleaned bottles were then double-bagged in clean plastic bags and placed in clean plastic storage containers for transport to the sampling site. Sampling was carried out from faucets on the wellheads of pumped boreholes; and boreholes were purged (typically more than 10 minutes) before sampling to obtain uncontaminated samples. The Hydrolab MiniSonde 5 with a flow-through cell was used to measure groundwater sample temperature, pH, specific conductance, and the oxidation-reduction potential (Eh). Water samples at each well site were allowed to flow through the Hydrolab MiniSonde 5 until equilibrium was reached. Dissolved oxygen, alkalinity (as HCO_3^-), N species, total Mn, total Si, Fe species and dissolved S^{2-} was determined using a portable spectrophotometer (HACH DR/890 Multi-Parameter Colorimeter).

In the field, two sample bottles were filled with groundwater; and a chemical reagent powder was dropped into one of the samples to test for a specific parameter. The greater the presence of a certain parameter, the stronger the color develops. The HACH spectrophotometer evaluates the light transmission through the sample, resulting in the amount of concentration of the specific parameter. For dissolved oxygen, two tests were used to measure concentration, High Range DO and Indigo Carmine method (low range). Estimated detection limit for DO is 18.8 $\mu molkg^{-1}$ for the High range method and 0.38 $\mu molkg^{-1}$ for the

Indigo Carmine method (HACH, 2009). Alkalinity (HCO_3^-) was determined by titration with a standard sulfuric acid solution to an end point pH, evidenced by the color change (HACH, 2009). Concentrations of dissolved NO_3^- and NH_4^+ were determined using the Cadmium Reduction method (detection limit 0.16 $\mu molkg^{-1}$) and Salicylate method (detection limit 0.55 $\mu molkg^{-1}$) respectively (HACH, 2009). Total manganese concentrations were determined by the PAN method, used to detect low concentrations of manganese (detection limit 0.13 $\mu molkg^{-1}$, HACH, 2009). Total silica and sulfide concentrations were measured using the Heteropoly Blue (detection limit 0.36 $\mu molkg^{-1}$) and Methylene Blue methods (detection limit 0.16 $\mu molkg^{-1}$), respectively (HACH, 2009). Ferrous iron (Fe^{2+}) concentrations were determined using the 1,10 Phenanthroline indicator with a detection limit of 0.36 $\mu molkg^{-1}$ (HACH, 2009). Total iron concentrations were measured by the FerroZine® method with a detection limit of 0.16 $\mu molkg^{-1}$ (HACH, 2009). Ferric iron (Fe^{3+}) does not react to the reagents, therefore Fe^{3+} concentration can be calculated by subtracting Fe^{2+} from the results of total iron concentrations.

4.2 Laboratory Approach

Groundwater samples were collected directly from the well head into collapsible "trace clean" Low-Density Poly-Ethylene (LDPE) cubitainers®. Samples were subsequently filtered through 0.45 μm in-line filter-capsules (Gelman Science, polyether sulfone membrane) and "trace clean" Teflon® tubing, using a peristaltic pump, into a 500 mL "trace clean" sample bottle. Samples were then acidified to a pH ~3.5 using ultra-pure HNO_3 (Seastar Chemical, Baseline) before transport back to the lab. Molybdenum concentrations were analyzed without preconcentration using a quadrupole inductively coupled plasma mass spectrometer (ICP-MS), located in the University of Texas at Arlington lab. A five-point calibration curve (0.01 ppb, 0.1 ppb, 1 ppb, 10 ppb, and 100 ppb) was used to constrain the sample Mo concentrations.

CHAPTER 5
RESULTS

Previous works have researched the Aquia Aquifer in the location of either the Eastern or Western Shore flowpath. In order to address the central hypothesis of the present study, Mo concentration, concentration and speciation of geochemical constituents, and solution composition are evaluated as a function of distance from the recharge zone for both the Eastern and Western Shore flowpaths. Specifically, the detailed assessment of the down-gradient trend in geochemical parameters will help define the behavior of Mo and its controlling factors along both flowpaths.

5.1 Eastern Shore Flowpath

Hydrogeochemical data for groundwaters from the Aquia Aquifer Eastern Shore flowpath are shown in Figures 4 and 5. Aquia groundwaters are near-neutral to slightly alkaline, with pH values ranging between 7.6 and 8.4. Alkalinity ranges from 2.0 to 4.2 mmol kg^{-1} (Table 2). Alkalinity and pH exhibit an overall increasing trend with down-gradient flow along the flowpath (Figure 4a & 4b). Dissolved oxygen (DO) concentrations range between 9.4 and 51 µmol kg^{-1} (Table 2). Dissolved oxygen concentrations are relatively low and decrease along flowpath (Figure 4c). Eh values range between -53 to 44mV and exhibit higher values near the recharge zone with a slight decrease further down-gradient along the flowpath (Figure 4d).

Total dissolved Fe concentrations (i.e., Fe_T) range from below detection to 17.7 µmol kg^{-1} (Table 3). Ferrous iron (Fe^{2+}) concentrations range from below detection to 9.9 µmol kg^{-1}, and Fe^{3+} concentrations range from below detection to 14.5 µmol kg^{-1} (Table 3). Beginning at the recharge area, Fe^{3+} predominates within the flowpath, whereas with flow beyond ~52 km, Fe^{2+} is the chief form of iron in the groundwater (Figure 5a). Dissolved sulfide (S^{2-}) concentrations range from below detection to 0.40 µmol kg^{-1} (Table 3). Sulfide concentrations

are inconsistent and are below detection in 6 out of 11 wells sampled along the Eastern Shore flowpath (Figure 5b). Dissolved total manganese (Mn) concentrations range from below detection to 1.02 μmol kg^{-1} (Table 3). Manganese concentrations are variable but exhibit a decrease down-gradient along the flowpath (Figure 5b). Dissolved nitrate (NO_3^-) concentrations range from below detection to 3.23 μmol kg^{-1} (Table 3), and in general exhibit low concentration along the flowpath, except at 52 km where NO_3^- displays its highest concentration (Figure 5c). Dissolved ammonium (NH_4^+) concentrations range from 0.42 to 15.1 μmol kg^{-1} (Table 3). Ammonium displays higher concentrations with flow beyond 36 km along flowpath and also exhibits higher concentrations than compared to NO_3^- (Figure 5c). Dissolved Mo concentrations range from 0.011 to 1.493 μmol kg^{-1} (Table 4). Molybdenum concentrations increase down-gradient along the flowpath (Figure 5d).

Table 2: Hydrogeochemical data of groundwaters from Aquia Aquifer for samples collected along the Eastern Shore flowpath in the summer of 2006 taken from Haque et al. (2008). Temperature (Temp), alkalinity as HCO_3 (Alk), pH, specific conductivity (Cond), total dissolved solids (TDS), oxidation-reduction potential (Eh), and dissolved oxygen (DO).

Sample	Distance Km	Temp ºC	Alk (HCO_3) mmol kg^{-1}	pH	Cond µScm	TDS mg kg^{-1}	Eh mV	DO µmol kg^{-1}
Eastern								
Shore wells								
KE-66-0125	22.5	16.6	1.99	7.57	222	143	25.5	51.0±1.80
QA-88-1277	33.5	15.6	2.79	7.69	296	189	44	13.5±0.21
QA-94-1322	36.2	18.6	3.08	8.01	330	211	-11	19.6±0.10
QA-88-1268	51.2	16.7	3.19	8.08	303	194	-10.5	16.8±0.07
State	52	19.7	2.91	8.38	305	196	-46	21.4±0.11
Hwy Admin								
QA-94-0111	52.5	16.2	3.79	7.91	366	234	-3	11.1±0.05
QA-95-0611	55	16.1	2.98	8.02	302	194	-18	50.0±0.00
QA-73-3626	64.5	16.9	3.46	7.84	351	213	27.5	23.3±0.12
QA-81-2298	70.7	17.5	3.79	8.3	296	189	-11	20.3±0.05
QA-92-0451	75.1	17.8	4.16	7.93	422	267	11.5	12.0±0.10
QA-EB-144	86.3	15.9	3.24	8.12	366	271	-53	9.38±0.08
Western								
Shore well								
AA-DE-218	40	14.5	2.48	7.81	300	192	60.5	124±1.80

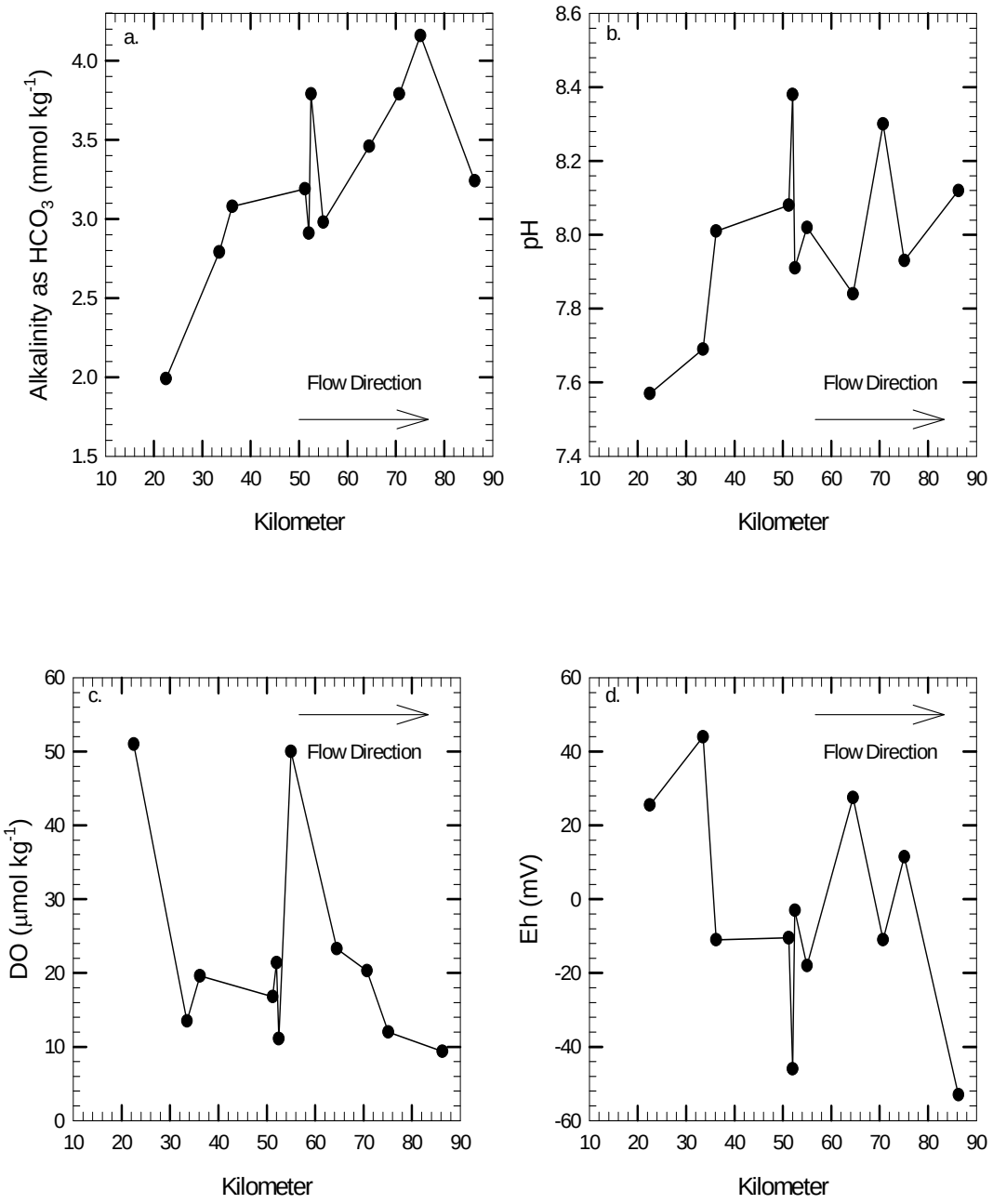

Figure 4: Aquia Aquifer data from the samples collected along the Eastern Shore flowpath in the summer of 2006 (Haque et al., 2008) (a) alkalinity; (b) pH; (c) dissolved oxygen; (d) Eh as a function of distance from recharge zone (km). (Modified from Haque, 2007)

Table 3: Concentrations and speciation data for dissolved Fe, S^{2-}, Mn, N, and Si in groundwaters samples collected from the Aquia Aquifer along the Eastern Shore flowpath in August of 2006 taken from Haque et al., (2008).

Sample	Distance Km	Fe_T µmol kg^{-1}	Fe^{2+} µmol kg^{-1}	Fe^{3+} µmol kg^{-1}	S(-II) µmol kg^{-1}	Mn µmol kg^{-1}	NO_3^- µmol kg^{-1}	NH_4^+ µmol kg^{-1}	Si mmol kg^{-1}
Eastern Shore wells									
KE-66-0125	22.5	12.7±0.21	0.90±0.03	11.8±2.58	BDL*	1.02±0.00	BDL‡	0.42±0.19	1.26±0.05
QA-88-1277	33.5	17.7±0.01	7.70±0.00	10.0±0.27	0.23±0.18	0.15±0.01	0.48±0.00	2.03±0.19	0.41±0.00
QA-94-1322	36.2	15.4±0.05	2.87±0.10	12.5±0.34	BDL	BDL†	1.13±0.00	14.8±0.00	0.32±0.00
QA-88-1268	51.2	14.7±0.08	0.18±0.00	14.5±0.39	0.10±0.18	0.42±0.01	0.32±0.00	9.12±0.93	0.44±0.00
State Hwy Admin	52.0	7.01±0.06	2.38±0.10	4.63±0.12	0.40±0.02	0.00±0.00	3.23±0.00	6.77±0.00	0.24±0.00
QA-94-0111	52.5	11.4±0.10	6.80±0.10	4.60±0.12	BDL	BDL	0.00±0.00	3.22±0.00	0.23±0.00
QA-95-0611	55.0	3.35±0.02	3.35±0.09	BDL°	BDL	BDL	0.76±0.09	4.83±0.00	0.57±0.00
QA-73-3626	64.5	BDL°	BDL¶	BDL	BDL	0.44±0.01	1.13±0.00	7.73±0.00	0.44±0.00
QA-81-2298	70.7	9.94±0.03	9.94±0.27	BDL	0.34±0.03	0.04±0.01	0.65±0.00	15.1±0.00	0.20±0.00
QA-92-0451	75.1	9.01±0.01	9.01±0.24	BDL	BDL	BDL	0.48±0.00	9.02±0.00	0.38±0.00
QA-EB-144	86.3	8.29±0.01	4.71±0.13	3.58±0.00	0.16±0.00	0.11±0.01	0.48±0.00	1.39±0.19	0.22±0.00
Western Shore well									
AA-DE-218	40.0	14.0±0.01	5.32±0.10	8.70±0.23	0.52±0.18	0.76±0.02	0.32±0.00	BDL∫	0.37±0.00

° BDL for Fe_T = 0.16 µmol kg^{-1} ‡ BDL for NO_3^- = 0.16 µmol kg^{-1} † BDL for Mn = µmol kg^{-1}

¶BDl for Fe^{2+} = 0.36 µmol kg^{-1} ∫ BDL for NH_4^+ = 0.55 µmol kg^{-1} *BDL for S^{2-} = 0.16 µmol kg^-

Table 4: Concentrations for dissolved Mo in groundwaters from the Eastern Shore flowpath of the Aquia Aquifer.

Sample	Distance (km)	Mo μmol kg^{-1}
Eastern Shore wells		
KE-66-0125	22.5	0.011
QA-88-1277	33.5	0.026
QA-94-1322	36.2	0.834
QA-88-1268	51.2	0.753
State Highway Admin	52	0.503
QA-94-0111	52.5	0.437
QA-95-0611	55	1.493
QA-73-3626	64.5	0.763
QA-81-2298	70.7	1.020
QA-92-0451	75.1	1.183
QA-EB-144	86.3	0.354

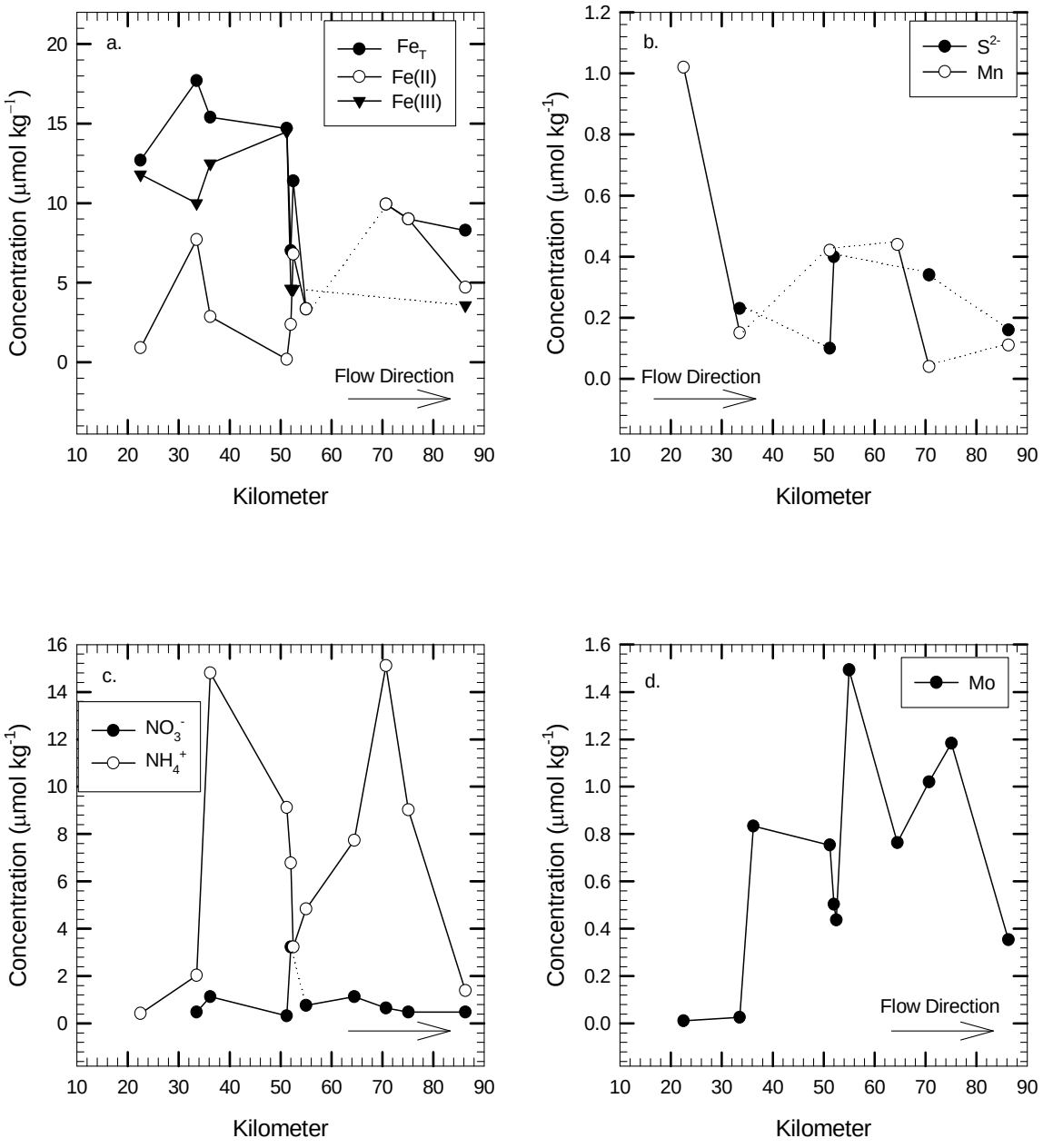

Figure 5: Aquia Aquifer data from the samples collected along the Eastern Shore flowpath in the summer of 2006 (Haque et al., 2008) (a) Fe speciation; (b) Mn and S^{2-} speciation; (c) N speciation; (d) dissolved Mo concentration as a function of distance from recharge zone (km). Solid lines are actual data and dotted lines represent values below the detection limit. (Modified from Haque, 2007)

5.2 Western Shore Flowpath

Hydrogeochemical data for groundwaters from the Aquia Aquifer Western Shore flowpath are shown in Figures 6 and 7. Aquia groundwaters are near-neutral to slightly alkaline, with pH values ranging between 7.8 and 9.7 (Table 5). Alkalinity (HCO_3^-) ranges from 1.6 to 5.1 mmol kg^{-1} (Table 5). Alkalinity displays relatively little change with a slight decrease in concentration down-gradient near the discharge locale, while pH exhibits an overall increasing trend with flow down-gradient along the flowpath (Figure 6a & 6b respectively). Dissolved oxygen (DO) concentrations range between 32.3 and 464 µmol kg^{-1} (Table 5). Dissolved oxygen concentrations are high and indicate oxic waters (i.e., O_2 > 30 µmol kg^{-1}) (Figure 6c). Measured Eh values range between -159 to 115 mV and support evidence of a reducing environment (Figure 6d).

Total dissolved Fe concentrations (i.e., Fe_T) range from 0.25 to 14.0 µmol kg^{-1} (Table 6). Ferrous iron (Fe^{2+}) concentrations range from below detection to 5.32 µmol kg^{-1}, and Ferric iron (Fe^{3+}) concentrations range from below detection to 8.70 µmol kg^{-1} (Table 6). Ferric iron displays a relative low concentration with the highest amount being reported at 40 km (8.70 µmolkg^{-1}, Table 6). At ~57 km Fe^{2+} becomes the dominant iron source for the remainder of the flowpath (Figure 7a). Dissolved sulfide (S^{2-}) concentrations range from below detection to 1.81 µmol kg^{-1} (Table 6). Sulfide concentrations are extremely low and are below detection in 10 out of 14 wells sampled along the Western Shore flowpath, except for an appearance at down-gradient distances of ~68-69km (Figure 7b). Dissolved total manganese (Mn) concentrations range from below detection to 1.41 µmol kg^{-1} (Table 6). Manganese concentrations are relatively low and show little change along the flowpath (Figure 7b). Dissolved nitrate (NO_3^-) concentrations range from below detection to 2.42 µmol kg^{-1} (Table 6), and in general, exhibit low but detectable concentration along the flowpath (Figure 7c). Dissolved ammonium (NH_4^+) concentrations range from below detection to 17.2 µmol kg^{-1} (Table 6). Ammonium displays higher concentrations in the groundwater as compared to NO_3^- (Figure 7c) which might suggest NO_3^- reduction. Dissolved

molybdenum (Mo) concentrations range from 0.085 to 0.461 µmol kg^{-1} (Table 7). Molybdenum concentrations increase down-gradient along the flowpath (Figure 7d).

Table 5: Hydrogeochemical data of groundwaters from Aquia Aquifer for samples collected along the Western Shore Flowpath in June of 2007. Well AA-DE-218, Western well collected in August 2006, is included in this table (Haque et al., 2008). Temperature (Temp), alkalinity as HCO_3 (Alk), pH, specific conductivity (Cond), total dissolved solids (TDS), oxidation-reduction potential (Eh), and dissolved oxygen (DO).

Sample	Distance (km)	Temperature ℃	Alk (HCO_3^-) mmol kg^{-1}	pH	Cond µScm	TDS mg kg^{-1}	Eh mV	DO µmol kg^{-1}
PG-81-1249	20	16.2	3.28	8.21	293	187	-1.0	82.3
CA-94-2719	23	15.6	1.84	8.43	300	190	-25	53.1
PG-81-0721	31	16.5	4.92	8.46	282	181	43	85.4
CA-73-3395	34	17.7	3.12	8.39	282	180	-15	139.0
AA-DE-218	40	14.5	2.48	7.81	300	192	61	124.0
CH-94-3169	44	17.2	2.16	8.38	257	165	3	32.3
CA-94-1194	45	16.9	2.32	8.43	293	188	23	95.8
CA-94-2436	57	18.5	5.12	8.48	290	185	-11	107.0
SM-94-2522	66	15.8	2.24	8.74	239	153	-58	78.1
SM-92-0701	68	17.3	1.60	9.01	214	137	-84	63.5
CA-88-3340	69	18.8	1.76	9.33	239	152	88	464.0
SM-81-0060	73	18.4	2.00	9.65	228	146	-159	69.8
CA-94-0409	74	18.9	2.72	9.49	271	174	-120	72.9
SM-81-2634	76	19.3	2.12	9.34	284	182	115	72.9

.

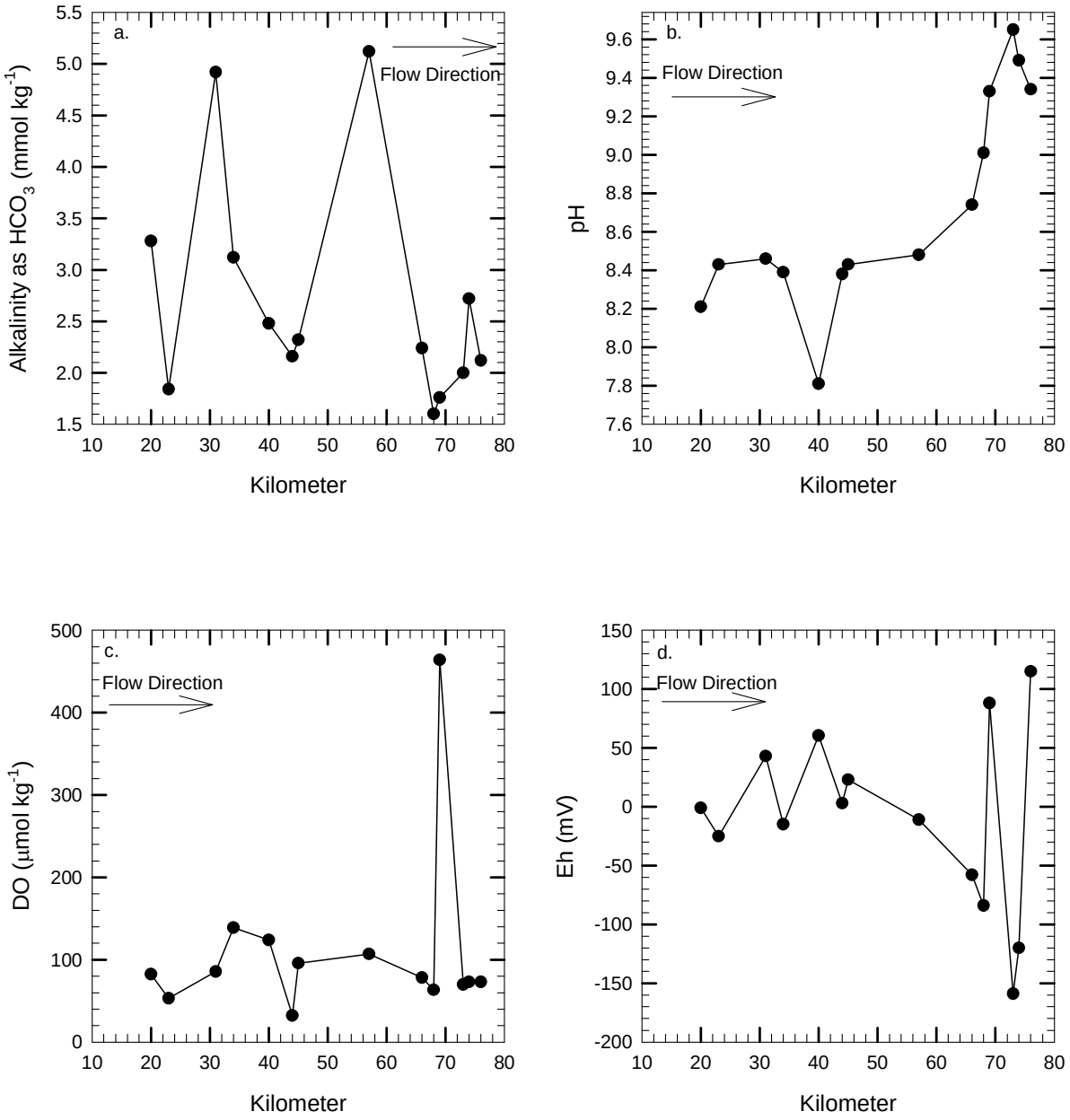

Figure 6: Aquia Aquifer data from the samples collected along the Western Shore flowpath in the summer of 2007 (Haque et al., 2008). (a) alkalinity; (b) pH; (c) dissolved oxygen; (d) Eh as a function of distance from recharge zone (km). Well AA-DE-218, Western well collected in August 2006, is included in this graph (Haque et al., 2008).

Table 6: Concentrations and speciation data for dissolved Fe, S^{2-}, Mn, N, and Si in groundwaters samples collected from the Aquia Aquifer along the Western Shore flowpath in June of 2007. Well AA-DE-218, Western well collected in August 2006, is included in this table (Haque et al., 2008).

Sample	Distance km	FeT µmol kg^{-1}	Fe^{2+} µmol kg^{-1}	Fe^{3+} µmol kg^{-1}	S(-II) µmol kg^{-1}	Mn µmol kg^{-1}	NO_3^- µmol kg^{-1}	NH_4^+ µmol kg^{-1}	Si mmol kg^{-1}
PG-81-1249	20	3.4	2.87	0.54	BDL*	0.02	0.22	11.4	0.18
CA-94-2719	23	2.96	1.79	1.17	BDL	1.22	1.83	5.28	0.16
PG-81-0721	31	1.83	1.85	BDL	BDL	0.59	1.56	6.46	0.21
CA-73-3395	34	1.58	1.01	0.57	BDL	BDL†	0.48	9.39	0.25
AA-DE-218	40	14.0	5.32	8.70	0.52	0.76	0.32	BDL∫	0.37
CH-94-3169	44	0.69	0.18	0.51	BDL	0.61	0.43	9.2	0.18
CA-94-1194	45	2.3	BDL¶	2.3	BDL	0.6	BDL‡	14.1	0.21
CA-94-2436	57	1.23	2.15	BDL	BDL	BDL	2.42	10.8	0.01
SM-94-2522	66	1.79	0.54	1.25	BDL	0.41	0.48	12.3	0.15
SM-92-0701	68	0.25	0.18	0.07	0.28	0.4	0.48	9.98	0.18
CA-88-3340	69	1.24	BDL	1.24	1.81	0.31	0.81	9.39	0.18
SM-81-0060	73	0.78	BDL	0.78	BDL	1.41	0.48	7.24	0.16
CA-94-0409	74	1.12	BDL	1.12	BDL	0.32	0.97	17.2	0.23
SM-81-2634	76	0.47	0.4	0.06	0.07	0.54	2.15	6.65	0.12

¶ BDL for Fe^{2+} = 0.36 µmol kg^{-1} ∫ BDL for NH_4^+ = 0.55 µmol kg^{-1} ‡ BDL for NO_3^- = 0.16 µmol kg^{-1}

* BDL for S^{2-} = 0.16 µmol kg^{-1} † BDL for Mn = µmol kg^{-1}

Table 7: Concentrations for dissolved Mo in groundwaters from the Western Shore flowpath of the Aquia Aquifer

Sample	Distance (km)	Mo $\mu mol\ kg^{-1}$
Western Shore wells		
PG-81-1249	20.0	0.181
CA-94-2719	23.0	0.122
PG-81-0721	31.0	0.135
CA-73-3395	34.0	0.258
AA-DE-218	40.0	0.085
CH-94-3169	44.0	0.332
CA-94-1194	45.0	0.147
CA-94-2436	57.0	0.186
SM-94-2522	66.0	0.409
SM-92-0701	67.5	0.342
SM-81-0060	73.0	0.441
CA-94-0409	74.0	0.454
SM-81-2634	76.0	0.461

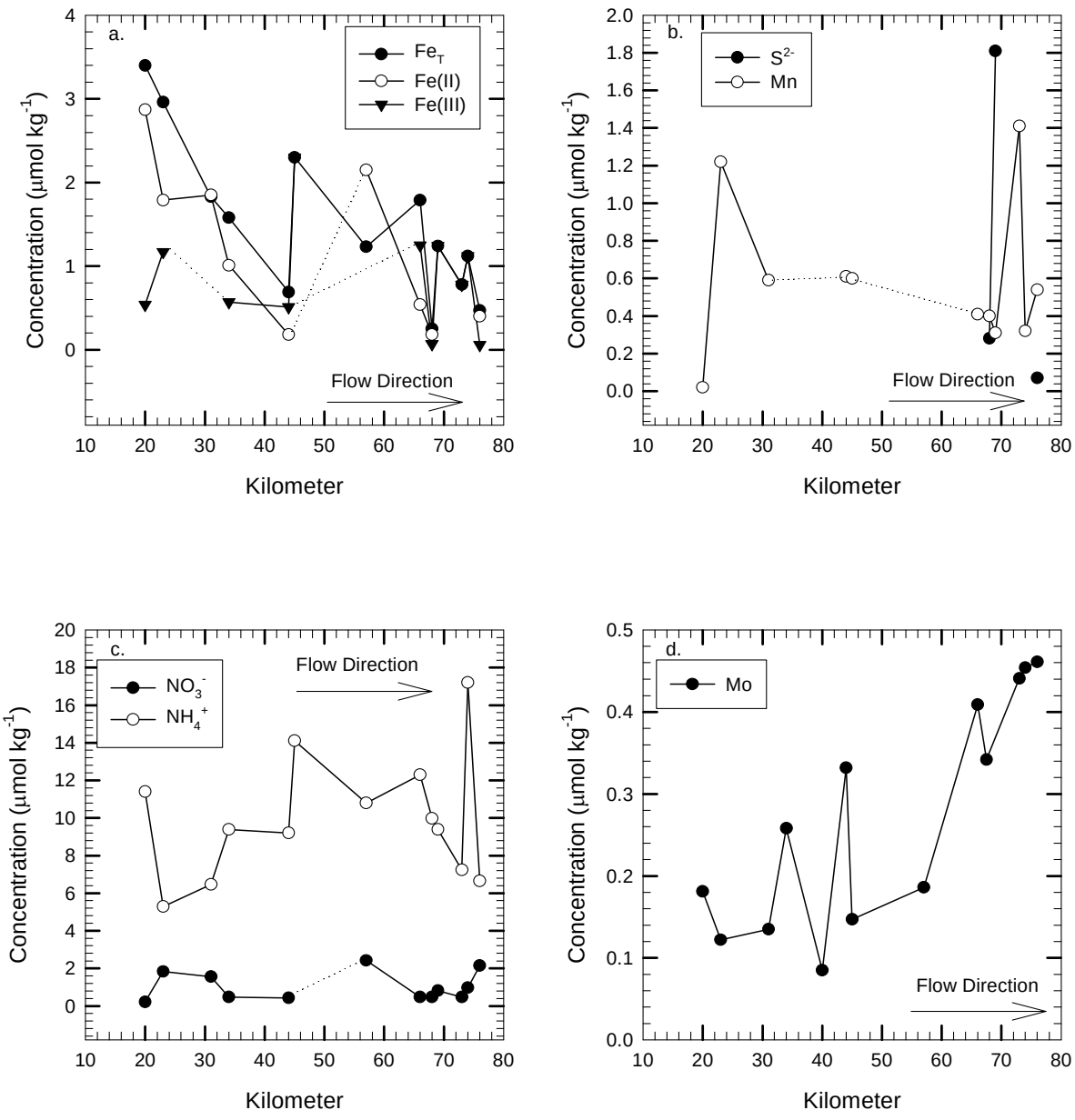

Figure 7: Aquia Aquifer data from the samples collected along the Western Shore flowpath in the summer of 2007 (a) Fe speciation; (b) Mn and S^{2-} speciation; (c) N speciation; (d) dissolved Mo concentration as a function of distance from recharge zone (km). Solid lines are actual data and dotted lines represent values below the detection limit.

CHAPTER 6
DISCUSSION

Confined groundwater systems, where the recharge zone is the only location that is open to atmospheric input, are characterized by a typical and predictable behavior. This type of system is known as the closed oxidant system (Champ and Gulens, 1978). Within this type of system, a dependable way to describe the chemistry behavior of the groundwater is to identify the oxidation/reduction (i.e., redox) processes. Oxidation/reduction gradients are viewed as a sequence of spatially distributed discrete zones, each dominated by a master electrochemical couple i.e., O_2/H_2O, NO_3^-/NH_4^+, Mn^{4+}/Mn^{2+}, Fe^{3+}/Fe^{2+}, SO_4^{2-}/H_2S, CO_2/CH_4 (Baedecker and Back, 1979; Champ et al., 1979; Chapelle, 1993; Groffman and Crossey, 1999). It is possible for redox zones to be tens of kilometers wide or only centimeters to millimeters wide in a regional flow system. Microbially produced enzymes have an effect on groundwater chemistry and the migration of chemical species in the Aquia Aquifer (Lovley and Chapelle, 1995; Lovley, 1997; Hunter et al, 1998). The consumption of electron acceptors (e.g., oxygen, NO_3^-, Mn(IV), Fe(III), SO_4^{2-} and CO_2) with the production of electron donors (e.g., NH_4^+, Mn(II), Fe(II), H_2S, and CH_4) along aquifer flowpaths (Kehew, 2001), is the most reliable way to identify redox zonation in aquifers where microbial activity is present. This paradigm represents a stable and predictable redox gradient in the aquifer from oxidizing conditions to more reducing groundwater along the flowpath.

6.1 Eastern and Western Shore Flowpath Comparison

The Aquia Aquifer is described as a closed oxidant system because atmospheric input is traditionally thought to only occur in the outcrop/subcrop portion of the aquifer. Knobel and others (1987) suggest that CO_2 is being produced by the metabolic activity of methanogenic

and sulfate-reducing bacteria. Chapelle (1983) suggest that CO_2 is being generated by the oxidation of lignite as a microbial by-product within the aquifer. In similar groundwater systems, the primary factor influencing the distribution and activity of microbial populations in an aquifer is the abundance and availability of reduced organics, inorganic nutrients and terminal electron acceptors (Champ and Gulens, 1978; Hunter et al., 1998; Vanbroekhoven, et al., 2007). The groundwaters of the Aquia initially contain oxidized species: O_2, NO_3^-, Mn^{4+}, Fe^{3+}, SO_4^{2-}, and CO_2 (Champ and Gulens, 1978; Chapelle and Knobel, 1983; Chapelle and Knobel, 1985). These oxidized species are documented to reduce to their lower redox couple in similar groundwater systems (e.g., H_20, NH^{4+}, Mn^{2+}, Fe^{2+}, H_2S, and CH_4) (Champ and Gulens, 1978; Hunter et al., 1998; Vanbroekhoven, et al., 2007).

Characteristically in most closed oxidant aquifers the onset of confined conditions are indicated by dissolved oxygen (DO) decreasing to near zero concentrations while pH and alkalinity (HCO_3^-) concentrations increase. Confined aquifers also display a decreasing trend in redox potential (Eh) along the flowpath. Aquifers which display reducing conditions are also characterized by an increase in the concentration of reduced constituents such as NH^{4+}, Mn^{2+}, Fe^{2+}, H_2S, CH_4 and HCO_3^- (Champ and Gulens, 1978; Morgan-Jones and Eggboro, 1981; Edmunds et al., 1982; Morgan-Jones, 1985; Hunter et al., 1998; Groffman, and Crossey, 1999; Brown et al., 2000). The results of Schlieker and others, (2001) show that the geochemistry of the trace elements involved can be explained to a large extent by the major redox processes of nitrate, manganese, iron, and sulfate; and in the case of the present study, increased concentrations of Mo along the flowpath may also be applied to support major redox processes along the flowpath of the Aquia Aquifer.

6.1.1 Alkalinity and pH

The Eastern Shore flowpath of the Aquia Aquifer is generally characterized by an increasing trend in alkalinity (HCO_3^-) (Figure 8a) and pH (Figure 8b), with pH values indicating near-neutral to slightly alkaline waters. In the Atlantic Coastal Plain Aquifer bicarbonate is typically the major dissolved anion (Chapelle and Knobel, 1985). Observed alkalinity

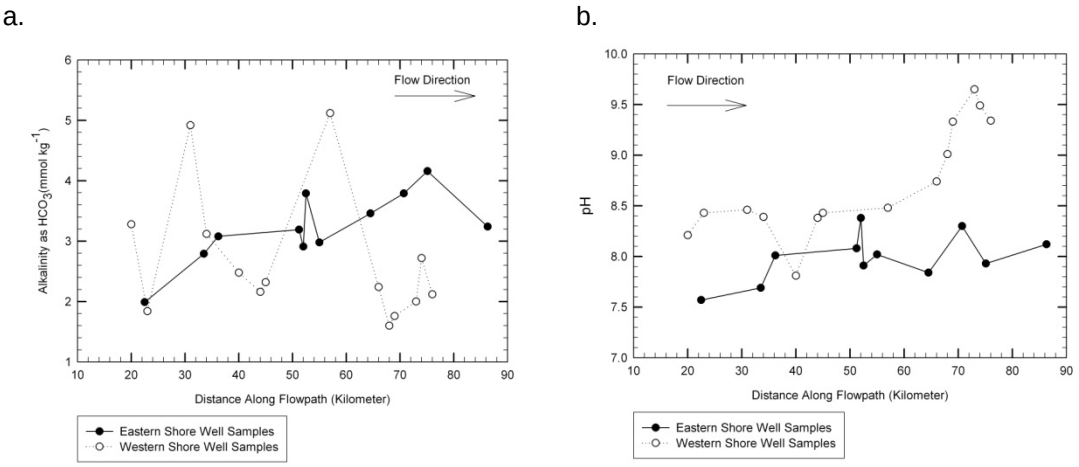

Figure 8: Comparison of the Aquia Aquifer data from the samples collected along the Eastern and Western Shore flowpath (a) alkalinity; (b) pH; as a function of distance from recharge zone (km).

concentrations along the flowpath of the Eastern and Western Shore is attributed to chemical weathering reactions and the dissolution of shell fragments that occur within the Aquia Aquifer (Chapelle and Knobel, 1983; Chapelle and Knobel, 1985), as well as an increase in carbon dioxide, which is generated in the aquifer by the oxidation of lignite (Chapelle, 1983). Bicarbonate concentrations can also increase due to microbial oxidation or bacterially mediated sulfate reduction (Chapelle et al., 1987; Purdy et al., 1992). With the use of ^{13}C data, Chapelle and Knobel (1985) discussed the sources and sinks of HCO_3^- along the flowpath of the Aquia Aquifer, and they concluded that more evolved waters containing isotopically heavy CO_2 are a by-product of bacterial mediated methanogenesis.

The data from the Western Shore flowpath exhibits increasing pH (7.8-9.7) along the flowpath (Figure 8b), while down-gradient alkalinity concentrations show relatively little change

with a slight decreasing trend near the discharge locale for the Western Shore flowpath (1.60-5.12 mmol kg^{-1}) (Figure 8a). One possible reason for this decline is indicated by potentiometric lows in the lower elevations near the Chesapeake Bay and Potomac River (Chapelle, 1983). Potentiometric lows in this region, suggest that some discharge of water is occurring and may be leaking into the formation above, the Marlboro Clay (Chapelle, 1983; Chapelle and Drummond, 1983; Purdy et al., 1987; Appelo, 1994; Purdy et al., 1996; Dai and Samper, 2006; Dai et al., 2006; Klohe and Kay, 2007), therefore, diluting the concentration of HCO_3^- with O_2-rich groundwater. A lack of microbial activity, resulting in a decline in CO_2 production, may be another reason for the decline in HCO_3^- concentrations at the south-east end (i.e., discharge locale) of the aquifer's flowpath. For both flowpaths the onset of confined conditions is reflected in an increase in pH at 42 km, which is related to changes in bicarbonate (alkalinity) and the beginning of ion-exchange reactions. The ion-exchange reaction occur when the Ca^{2+} is actively replaced by Na^+ at ~42km and down-gradient along flow, and where calcium carbonate precipitation is no longer an effective buffer control resulting in an increase in pH (Morgan-Jones and Eggboro, 1981). This is evident in the flowpath water chemistry change from a Ca-Mg bicarbonate type to a Na^+ bicarbonate type, where glauconite acts as the exchange medium (Chapelle and Knobel, 1983; Chapelle and Knobel, 1985; Knobel et al., 1987;).

6.1.2 Dissolved Oxygen

Dissolved oxygen content (9.4-51 μmol kg^{-1}) along the Eastern Shore, near the recharge zone, defines an oxic environment (i.e., O_2 > 30 μmol kg^{-1}), while 30 km along the flowpath, DO concentrations reveal a more suboxic environment (i.e., 1 μmol $kg^{-1} \leq O_2 <$ 30 μmol kg^{-1}) (Figure 9a). A gradual depletion of DO in the confined region of the aquifer reflects bacterial demand and oxidation of pyrite and other ferrous minerals (Edmunds and Walton, 1983). This region of reduced oxygen content infers the onset of confinement within the aquifer. The Western Shore flowpath DO content (32.3-464 μmol kg^{-1}) defines a more oxic environment (i.e., O_2 > 30 μmol kg^{-1}) along the entire length of the aquifer (Figure 9a). The oxygen content of

the Western Shore flowpath suggests that the aquifer is leaky, and oxygen is being replenished by the upper formation, Marlboro Clay (Chapelle, 1983; Chapelle and Drummond, 1983; Purdy et al., 1987; Appelo, 1994; Purdy et al., 1996; Dai and Samper, 2006; Dai et al., 2006; Klohe and Kay, 2007).

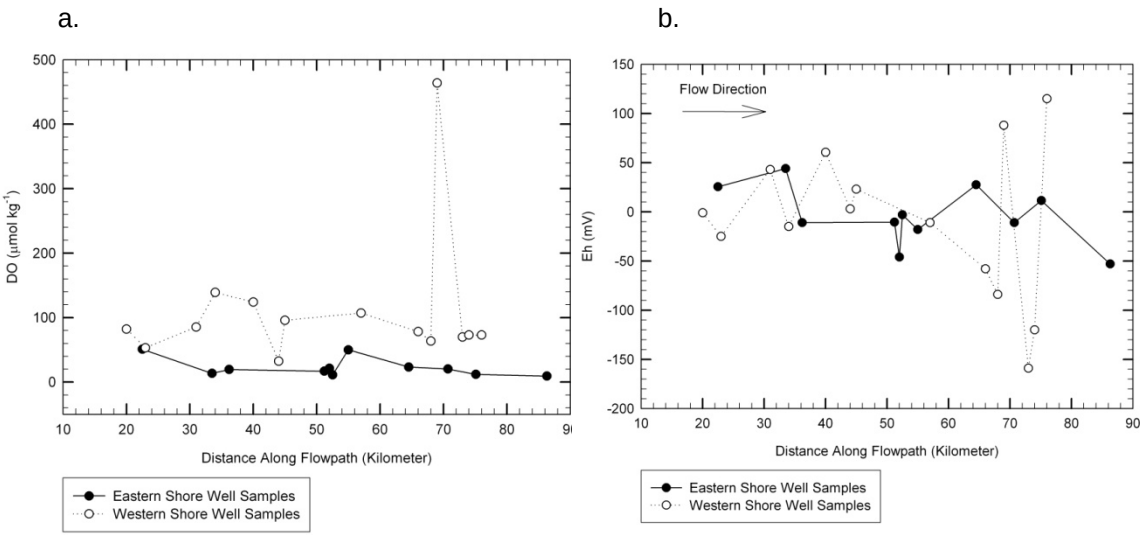

Figure 9: Comparison of the Aquia Aquifer data from the samples collected along the Eastern and Western Shore flowpath (a) dissolved oxygen; (b) Eh (mV); as a function of distance from recharge zone (km).

6.1.3 Redox Potential

Decreasing Eh values along the direction of groundwater flow is due to the oxidation of sedimentary organic materials (Champ and Gulens, 1978), and defines strongly reducing environments for both the Eastern and Western Shore flowpaths of the Aquia. Redox potential is used as a qualitative indicator of reduction potential because of the ongoing microbial processes that occur in the aquifer. Redox potential (Eh) (53-44mV) in the Eastern Shore flowpath, decreases further down-gradient, supporting evidence of an increasingly reducing environment (Figure 9b). Eh levels in the Western Shore flowpath (-159-115mV) do not decrease along flowpath (Figure 9b), but Eh levels do reveal a discrete zone where Eh was

measured to be negative at ~57km, which coincides with Fe^{3+} reduction. Furthermore, a marked decrease in redox potential (Eh) of 247mV at ~70km along the flowpath may coincide with sulfate reduction. In the case of both the Eastern and Western Shore flowpaths, Eh measurements show a marked decline in potential between 40 and 70 km along the flowpath. This zone of reduction can be associated with the appearance of the reduced form of iron (Fe^{2+}), sulfur (S^{2-}), and nitrogen (NH_4^+), and an increase in concentrations of total manganese and molybdenum in both flowpaths.

6.1.4 Nitrate and Ammonium

Nitrate concentrations are considered to be low, but measurable, along the Eastern and Western flowpaths of the Aquia Aquifer. It is not clear whether these confined groundwaters have ever contained substantial amounts of NO_3^- because of their geologic age. A decrease in NO_3^- along both aquifers is the result of denitrifying bacteria (Lovley and Chapelle, 1995; Hunter et al, 1998; Penny and Lee, 2003; Vanbroekhoven et al., 2007; Figure 10a & 10b). Ammonium also decreases at the discharge locale of both flowpaths due to microbial activity. There is an inverse relationship between NO_3^- and NH_4^+ along both flowpaths and NH_4^+ concentrations are greater in relation to NO_3^-. This inverse relationship suggests that the reduction of NO_3^- has led to the generation of NH_4^+ (i.e., dissimilatory nitrate reduction, Figure 8a and 8b, Eastern and Western flowpath, respectively). Nitrate and NH_4^+ concentrations are variable throughout the flowpath for both the Eastern and Western Shore, therefore, identifying a discrete nitrate redox zone is not possible.

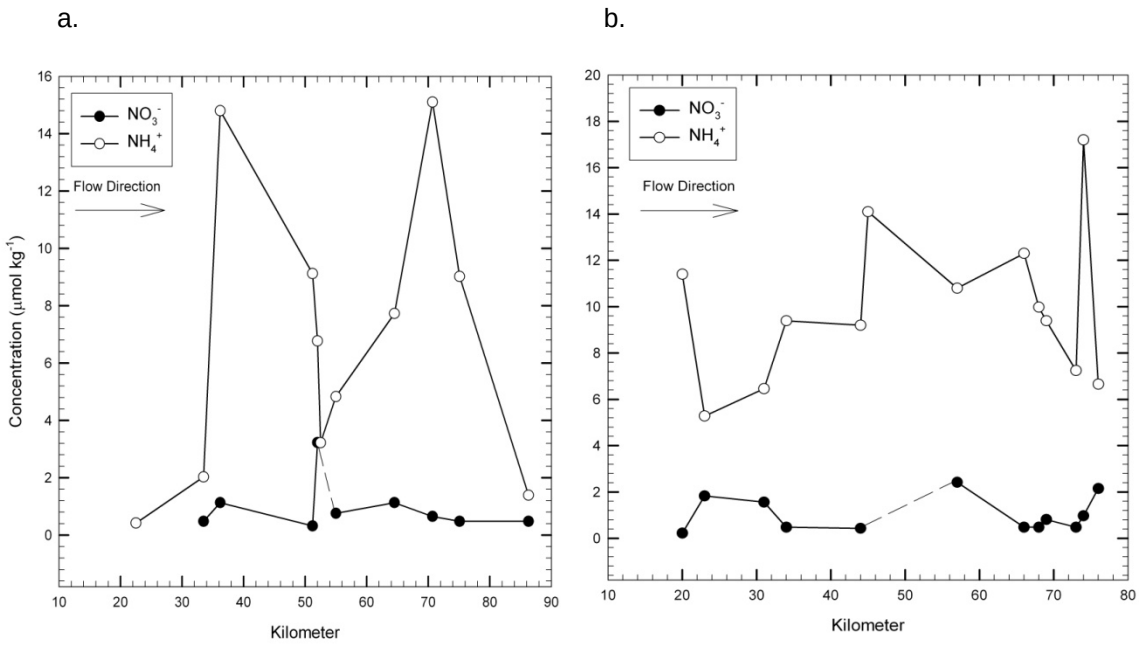

Figure 10: Comparison of nitrate and ammonium concentrations along the Eastern (a) and Western (b) Shore flowpaths in the Aquia Aquifer as a function of distance from recharge zone (km). Solid lines are actual data and dotted lines represent values below the detection limit

6.1.5 Total Manganese

Total manganese values are low for the Eastern Shore flowpath and are typically below detection limit, reflecting the low solubility of Mn(IV) minerals (Smedley and Edmunds, 2002). Concentrations of Mn along the Western Shore flowpath are mostly above the detection limit. Concentrations of Mn decrease gradually along both the Eastern and Western flowpaths which may be the product of a preferred reduction by dissimilatory bacteria, if the assumption is made that Mn exists in the oxidized form, Mn(IV) (Postma and Jakobsen, 1996). Microbial reduction of Mn may not occur based on the fact that Mn-hydroxides can be rapidly removed to the sediments *via* precipitation and organisms must have the ability to either solubilize the substrate or have the ability to transport the substrate into the cell as a solid (Nealson and Myers, 1992).

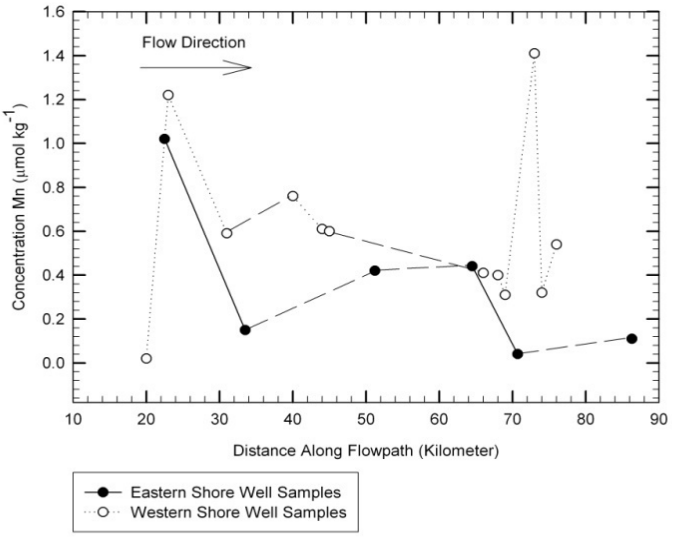

Figure 11: Comparison of the Aquia Aquifer data from the samples collected along the Eastern and Western Shore flowpath Manganese; as a function of distance from recharge zone (km).

The gradual decrease in concentration can also represent the precipitation/sorption of Mn-hydroxides, due to the contrast in Eh-pH conditions, onto the mineral surface of clay found in the Aquia (Schurch, et al., 2004).

6.1.6 Iron

Iron reduction is an important indicator of redox conditions. High concentration of iron at the recharge zone along the Eastern Shore flowpath suggests Fe^{3+} reduction. Well site, QA-94-0111 located 52.5 km from the recharge zone, distinguishes this Fe^{3+} reduction (Figure 12a). Ferrous iron is commonly present in groundwater within the moderate (6-8) pH range coupled with a low Eh (-46 mV) (Kehew, 2001).

In comparison, initiation of Fe^{3+} reduction appears in the Western Shore flowpath at ~42km down-gradient of the recharge area. At well site CA-94-2436, located 57 km down-gradient of the recharge zone reveal Fe^{2+} concentrations measured at 2.15 μmol kg^{-1}, while Fe^{3+} concentrations are below detection limit. Consequently, pH values are moderate to high (8.5) and Eh measures relatively low (-11 mV). The Fe^{3+} reduction zone is evident at ~57 km down-gradient of the recharge zone. An increase in HCO_3^- concentrations at 57 km, supports bacterial reducing microbes such as (*Geobacter sp*. and *Shewenella putrifaciens*) which utilize

Fe^{3+} oxides as an electron acceptor to oxidize organic matter and result in an increase in Fe^{2+} (Haque, 2007). After ~ 69 km, Fe^{2+} concentrations were measured below detection limits. This indicates that Fe^{3+} reduction is not active in down-gradient of ~69 km in the aquifer.

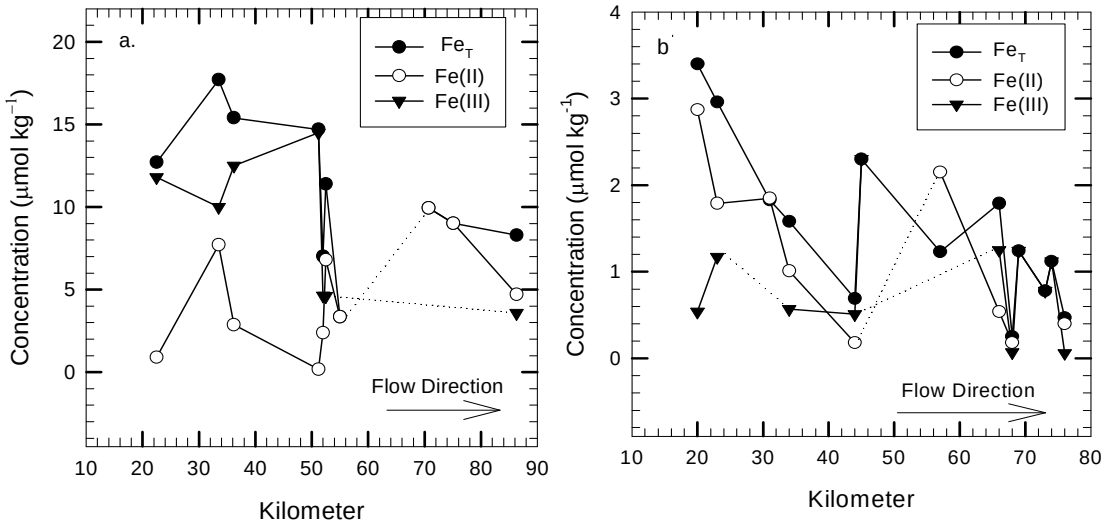

Figure 12: Comparison of Fe speciation from the Aquia Aquifer data from the samples collected along the Eastern (a) and Western (b) Shore flowpath; as a function of distance from recharge zone (km).

6.1.7 Sulfide

After iron reduction is complete, sulfate reduction occurs by sulfate-reducing consortia. Sulfate-reducing zones are recognized by the decrease in sulfate and/or the production of sulfide (Jackson and Patterson, 1982). In the Eastern Shore flowpath, concentrations of S^{2-} are low and in many well sites are below detection limits. Pyrite is commonly found in the Aquia Aquifer (Chapelle and Knobel, 1983). The formation of pyrite can occur in environments where Fe^{2+} increases with the presence of dissolved S^{2-} concentrations. This type of condition may occur at ~70.7km from the recharge zone where Fe^{2+} concentrations are at their highest (9.94 ± 0.27 μmol kg^{-1}, Figure 13b) and S^{2-} concentrations are measured at 0.34 ± 0.03 μmol kg^{-1} (Figure 13a). Increasing concentrations of S^{2-} may also result in the scavenging of metal

cations therefore, reducing concentration of trace-metals (e.g., Mo) (Vanbroekhoven et al., 2007).

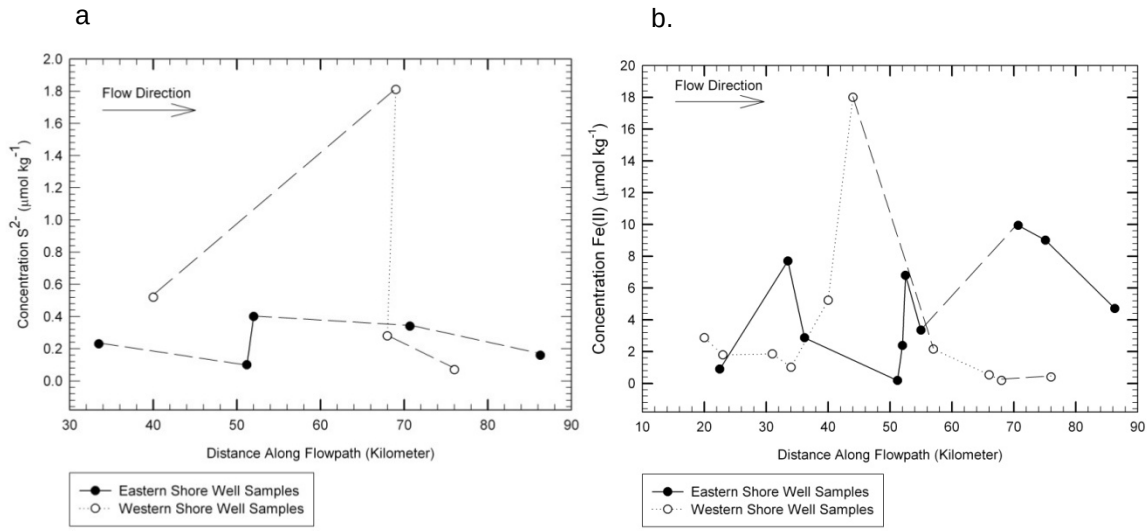

Figure 13: Comparison of the Aquia Aquifer data from the samples collected along the Eastern and Western Shore flowpath (a) Sulfide; (b) Fe^{2+}; as a function of distance from recharge zone (km).

Sulfide concentrations in the Western Shore flowpath are similar in comparison to the Eastern Shore flowpath. Ten out of fourteen wells are measured at below detection limits (Table 6). The lack of sufficient availability of Fe^{2+} in the down-gradient flow, suggest that there is no pyrite formation occurring in the south-east end of the Western Shore flowpath.

6.1.8 Molybdenum

Molybdenum is an important trace metal and indicator of redox reactions within both the Eastern and Western Shore flowpaths. Molybdenum reveals an increase in concentration along the Eastern Shore flowpath (0.011- 0.354 μmol kg^{-1}, Table 4) and the Western Shore flowpath (0.181 – 0.461 μmol kg^{-1}, Table 7), but the behavior of Mo varies slightly between the two flowpaths. In the Eastern Shore flowpath, Mo concentrations are relatively higher and in the Western Shore flowpath, a conservative behavior of Mo is more evident. The conservative behavior can be explained by an increasing pH (Figure 2b) which prohibits desorption of Mo from iron and manganese oxides; the relative higher concentrations are the result of decreasing

Eh (Figure 2d) which provides the reduction potential of Fe and Mn oxy-hydroxides, which is driven by microbial activity, permitting desorption of Mo, and finally releasing Mo into solution.

Beginning near the recharge zone along the Eastern Shore at well site KE-66-0125, 22.5 km from the recharge zone, Mo is measured at its lowest concentration (0.011 μmol kg^{-1}, Figure 14). At near neutral pH (~7.6) conditions, sorption of Mo onto positively charged surface sites of Fe oxy-hydroxides, clay minerals, and/or organic matter may result in lower concentration of Mo in solution. At well site QA-95-0611 located 55 km from the recharge zone along the Eastern Shore flowpath, Mo concentration increases to a maximum of 1.493 μmol kg^{-1} (Figure 14). This increase is the result of pH (> 8.0, Figure 2b) induced desorption/dissolution and microbial dissimilatory reduction of iron and sulfate. Down-gradient at ~80 km from the recharge zone, low concentration of Mo (0.354 μmol kg^{-1}, Table 4) coincide with detectable concentration of S^{-2} (0.16 $\pm$ 0.0 μmol kg^{-1}, Table 3) and relatively high concentrations of Fe^{2+} (9.01 $\pm$ 0.24 μmol kg^{-1}, Table 3). Relatively low concentration of Mo may be explained by the formation of pyrite where Mo in solution is being co-precipitated/re-adsorbed with the newly formed Fe^{2+} sulfides.

Along the Western Shore flowpath at approximately 60 km from the recharge zone, Mo shows an increase (0.186 to 0.409 μmol kg^{-1}, Table 7), which correlates with the reduction of Fe^{3+}. At sites beyond 70 km, Mo increases to its highest concentration (0.461 μmol kg^{-1}, Table 7). This increase in concentration is the result of pH levels being greater than 9.0, a decrease of Eh (88 to -159 mV), and microbial iron and sulfate reduction occurring. When comparing the two flowpaths Mo behaves in a similar way, increasing in concentration along the flowpath while also supporting evidence of reducing conditions and microbial mediated processes. On the Eastern Shore the behavior of Mo is controlled by the microbial mediated reduction of iron oxy-hydroxides and the co-precipitation of FeS_2. While in the Western Shore the behavior of Mo is controlled by the microbial mediated reduction of iron and sulfate.

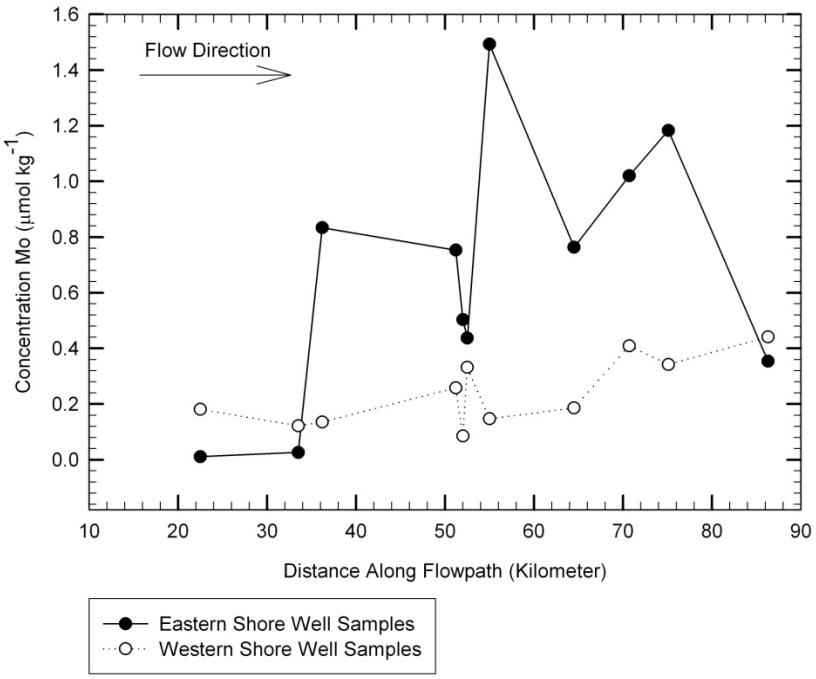

Figure 14: Comparison of Mo from the samples collected along the Eastern and Western Shore flowpath of the Aquia Aquifer as a function of distance from recharge zone (km).

6.2 Comparison of the Aquia Aquifer With Aquifers That Demonstrate Similar Behavior

The Aquia Aquifer is described as a confined hydrostratigraphic unit and a closed oxidant system (Chapelle and Knobel, 1983; Knobel et al., 1987). Similar type aquifers from around the world are used in comparison to facilitate a better understanding of the down-gradient behavior of the Aquia Aquifer. The Jurassic Lincolnshire Limestone located in Gloucestershire, England, is a well-studied example of a confined aquifer that resembles a closed oxidant system (Champ and Gulens, 1978; Morgan-Jones and Eggboro, 1981; Edmunds and Walton, 1983; Bottrell et al., 2000). The Lincolnshire aquifer is a carbonate aquifer (Morgan-Jones and Eggboro, 1981; Edmunds and Walton, 1983). Although the Aquia is predominantly quartz sand, there is a significant amount of calcite in solution due to the presence and dissolution of calcite and aragonite shells which make up about 2 to 20% of the aquifer material (Chapelle and Knobel, 1985). The Lincolnshire displays similar behavior in

hydrogeochemical processes. A gradual change in water chemistry from a Ca-HCO_3^- to a Na-HCO_3^- type water is similar to the change in the Aquia where groundwater in the outcrop area is Ca-Mg-HCO_3^-, which gradually evolves to a Na-HCO_3^- water down-gradient (Morgan-Jones and Eggboro, 1981; Chapelle and Knobel, 1983). The cation-exchange reaction where most of the Ca^{2+} is exchanged with Na^+ and where calcium carbonate precipitation is no longer a buffer control, water chemistry results in pH levels increasing along the Lincolnshire flowpath (Champ and Gulens, 1978; Morgan-Jones and Eggboro, 1981). The cation-exchange reaction almost coincides with the redox boundary which is detected around 12 km from the outcrop in the Lincolnshire (Edmunds and Walton, 1983). The process of ion-exchange in the Aquia is also defined by the replacement of Na^+ on glauconite which acts as a reactive exchange site. This chemistry change coincides with the redox boundary found for both the Eastern and Western Shore flowpaths.

The hydrogeochemical evolution along the flowpath within the Lincolnshire Limestone aquifer system suggests that the identification of three redox zones may exist: oxygen-nitrate, iron-manganese, and sulfide zones (Champ and Gulens, 1978; Morgan-Jones and Eggboro, 1981; Edmunds and Walton, 1983; Bottrell et al., 2000). Groundwater entering the flow system from the recharge area in the shallow confined zone of the aquifer contains both dissolved oxygen and nitrate; and has been characterized as the oxygen-nitrate redox zone (Champ and Gulens, 1978). Downdip of the recharge zone, approximately 4 km, Morgan-Jones and Eggboro (1981) research confirmed a depletion of dissolved oxygen. Approximately 11-12 km downgradient of the recharge zone, Eh measurements were reported to rapidly decrease causing the groundwater to become a reducing environment (Champ and Gulens, 1978; Edmunds and Walton, 1983). Ferrous iron is reported to increase in concentration in the reducing zone ($Fe^{2+} > 8.95$ μmol kg^{-1}) but once sulfide is produced much of the Fe^{2+} is removed as ferrous sulfide (Edmunds and Walton, 1983). The sulfide zone is thought to occur after the reduction of iron and manganese (~16km from the recharge zone) (Champ and Gulens, 1978).

The groundwater in this zone becomes adequately reducing allowing the production of sulfate-reducing bacteria (Champ and Gulens, 1978).

The data from the Aquia Aquifer differs from that of the Lincolnshire because the Aquia does not reveal three distinct zones of reduction. The Eastern and Western Shore flowpaths behave in the same way and resemble the Lincolnshire, but due to the large recharge zone of the Aquia Aquifer, there is evidence of a poorly-defined oxygen-nitrate redox zonation. Oxygen and nitrate are at detectable concentrations throughout the aquifer. Eh/pH relationships reflect the reduction of iron and sulfate. Along the Eastern Shore flowpath Eh levels begin to decrease at ~52 km downgradient of the recharge area while pH levels show to be at the highest reading (8.38). This provides a reducing environment where Fe^{2+} becomes the dominant source of iron (Fe^{2+} < 2.4 μmol kg^{-1}). Based on the presence of sulfide (Jackson and Patterson, 1982) and extremely reducing water the sulfate reduction zone appears to take place down-gradient of the iron reduction zone in the Eastern Shore. Along the Western Shore flowpath the appearance of sulfide is marked by a decrease in Eh potential of 88 to -159mV, therefore, the sulfate-reduction zone is occurring (1.81 μmol kg^{-1}) at ~70 km down-gradient.

The Rio Calaveras is a shallow aquifer located in the Jemez Mountains of northern New Mexico. The aquifer differs from the Aquia because residence time is short and velocities are generally high, but in comparison, the aquifer demonstrates overlapping redox zones in the presence of oxic and suboxic water. This overlap of redox zones is apparent in regions of the aquifer where iron and manganese exist in the presence of molecular oxygen and in zones where sulfate and iron reduction take place simultaneously (Groffman and Crossey, 1999). The hydrochemical data define a dominant redox potential shift spatially and temporally from O_2/H_2O_2 during spring to a Fe^{3+}/Fe^{2+}, Mn^{4+}/Mn^{2+} and SO_4^{2-}/HS^- system with the onset of summer.

Results of the Rio Calaveras aquifer work indicate that DO concentrations are higher during conditions of spring snow melt (May) and lower during conditions of autumn base flow

(September). The distribution of iron in shallow ground water has an inverse relationship with that of oxygen. Ferrous iron above 17.9 μmol kg^{-1}, reacts as a redox buffer maintaining low concentrations of oxygen and selectively reducing manganese; this is evident at the top of the water table where ferric oxidation products form, thus providing evidence for a mixed redox environment (Groffman and Crossey, 1999). Manganese exhibits low concentrations in the Rio Calaveras aquifer but persists in groundwater under both suboxic and weakly oxidizing environments. Sulfate concentrations also fluctuate throughout an annual cycle, where during the summer, sulfate reduction have been documented to reduce concurrently with iron reduction.

The Rio Calaveras Aquifer evolution is similar to both flowpaths in the Aquia Aquifer. The presence of DO in the Rio Calaveras Aquifer flowpath is similar to the Aquia Eastern Shore flowpath, which exhibits an oxic to suboxic system, and the Western Shore flowpath, which reveals oxic conditions. Similarly to the Aquia, iron and sulfate reduction can only occur in discrete zones where suboxic or dysoxic environments exist. Comparing the similarities and differences of the Aquia with other aquifers of similar parameters can support the interpretation this study has offered on both flowpaths of the Aquia Aquifer.

6.3 Utility of Molybdenum as a Groundwater Tracer

The behavior of Mo can be used in a variety of ways in a groundwater study: (1) Mo concentrations can be used to examine groundwater flowpaths to evaluate the potential for an inorganic contamination front, used in water quality assurance studies (Hearne and Litke, 1987; Hodge et al., 1996; Edmunds et al., (2002); Leybourne and Cameron, 2008); (2) Mo concentrations can be used to identify ferric hydroxide-ferrous ion redox processes (Hem, 1977; Smedley and Edmunds, 2002); and, (3) Mo concentrations can be used to indicate residence time in groundwaters (Edmunds and Smedley, 1998). Molybdenum is used in the present study because it can be measured in the aqueous phase with sufficient accuracy; and, Mo displays

significant changes in concentration with changing redox conditions, which suggest the location of redox boundaries.

Hearne and Litke (1987) conducted a groundwater flow and quality study near Canon City, Colorado. The report focused on aquifers that underlie the Lincoln Park area, which contained measurable concentrations of contaminants that are similar to the liquid waste produced by a nearby uranium-ore processing mill. Hearne and Litke (1987) collected and analyzed water samples from 28 sites for major and trace elements. Chemical constituents that were measured to determine the extent of the contamination were molybdenum, selenium, and uranium, which occur in large concentrations in raffinate (liquid waste) waters from the mill (Hearne and Litke, 1987). They concluded that none of the samples from deep wells contained significantly large concentrations of raffinate components, but shallow wells had higher concentrations. Therefore, the deep migration path within the studied formation was less important than a shallow migration path, which provided the route for the migration of raffinate-affected water (Hearne and Litke, 1987).

Molybdenum, as well as Re and U concentrations were analyzed in the groundwaters located in the Ash Meadow National Wildlife Refuge in southern Nevada and Death Valley National Park in eastern California (Hodge et al, 1996). The study site was prompted by the close proximity of the Nevada Test site, and the proposed high-level waste repository planned for Yucca Mountain. Because of geochemical similarities between naturally dissolved Re and Tc, which is present in fallout from nuclear weapons testing, and occurs in high-level radioactive wastes from nuclear power plants, understanding the behavior of Re assists in the prediction of the potential for groundwater transport of Tc (Hodge et al., 1996). Similar geochemistry of Re, Mo, and U in seawater prompted the measurement of Mo and U concentrations in all groundwater samples.

The groundwaters of the Great Basin, the study site, are reported to be fully oxygenated (Hodge et al., 1996). The study concluded that because of a positive correlation of the trace

metals Re, Mo, and U with each other and with Na, SO_4^{2-}, and Cl in all groundwater samples, that these trace constituents behave conservatively under oxic conditions. Consequently, these trace metals may prove to be effective in identifying groundwater flowpaths and evaluating the potential for contamination of the regional groundwaters with the groundwaters from the Nevada Test Site that may have interacted with radionuclides.

Flowpath evolution in groundwaters of the Spence Deposit in northern Chile was evaluated by studying the source of Mo and its interactions with other metals and metalloids (Leybourne and Cameron, 2008). Groundwater samples were collected along a flowpath through an undisturbed porphyry copper deposit (Spence deposit) to determine 1) the sources of elevated metals and metalloids, 2) the style of water-deposit interaction occurring along the flowpath, 3) the extent of transport of porphyry-associated metals and metalloids, and, 4) the mechanisms of metal and metalloid reduction. To accomplish these objectives, samples were measured for concentrations of metals and metalloids, which included Cu, Se, Re, Mo, and As. Groundwaters up-gradient of the deposit represent regional groundwaters with relatively low concentrations of metals and metalloids, characteristic of the Cu ores in northern Chile (Leybourne and Cameron, 2008). Ore-related metals, metalloids, and SO_4^{2-} were elevated within and down-flow of the deposit (Se up to 10.13 μmol kg^{-1}, Re up to 0.17 μmol kg^{-1}, Mo up to 4.95 μmol kg^{-1}, and As 4.00 μmol kg^{-1}). The source of this elevated concentration is the result of water-deposit interaction, yielding metals and metalloids that are characteristic of porphyry Cu deposit. Copper and other metal cations (e.g., Pb, Zn, Ni, and Co) concentrations were elevated within the deposit, but decreased in concentration down-gradient of the deposit. Leybourne and Cameron (2008) concluded that elevated concentrations of SO_4^{2-}, Se, Re, Mo, and As, down-gradient the Spence deposit, are due to the behavior of these elements which act as anions or neutral species as a result of Eh-pH conditions of the groundwaters, which results in their mobility. Base metals (Cu, Pb, Zn, Ni, and Co) measured down-gradient of the Spence deposit, display decreasing concentrations in comparison with the former group (Leybourne and

Cameron, 2008). These base metals are presented as cations and Leybourne and Cameron (2008) concluded that the decrease in concentration is the result of adsorption to colloidal material.

Edmunds and others (2002) investigated the geochemical evolution of groundwater beneath Mexico City. The main objective was to identify chemical changes taking place along the original direction of groundwater flow and detect the extent of contaminant inputs from Mexico City to the confined parts of the aquifer. In order to accomplish this objective, the researchers used stable isotopes, radiocarbon and major/minor trace elements. The aquifer system is marked by a change in redox potential (Eh) of over 200 mV ~12 km down-gradient of the flowpath. The change from oxidizing to reducing conditions is accompanied by a distinct change in elemental concentrations, for example, the increase in Fe^{2+} from below 2.00 µmol kg^{-1} to above 4.00 µmol kg^{-1}. Manganese concentrations are low in the aerobic section but show an increase before the redox boundary and thereafter. Manganese concentrations continue to increase in the anaerobic groundwater. They concluded that this reflects the stability range of Mn^{2+} which is considerably larger than Fe^{2+}. Molybdenum was used as a minor trace element in this study. "Molybdenum, like the other oxyanion-forming elements also showed an increase to around 6 µmol kg^{-1} in the aerobic groundwater but then maintained high concentrations throughout the anaerobic section" (Edmunds et al., 2002, p.16). Edmunds and others (2002) concluded that this is in accordance with trends found in sedimentary aquifers where Mo accumulates in shallow groundwaters with increasing residence time. In this particular example Edmunds and others explained that Mo may have also increased in concentration due to increasing temperature under the reducing conditions of the aquifer.

Metals such as Cu, Ag, and Cr in groundwaters, may be lowered by the chemical reduction involving ferric hydroxide-ferrous ion redox processes. In addition, Mo concentrations may provide a proxy for these processes. Hem (1977) investigated the reactivity of freshly precipitated and disordered ferric hydroxide and manganese oxides in terms of chemical

oxidation and reduction. Hem provides Eh-pH diagrams and/or solubility graphs for nine elements whose chemical behavior may be influenced by reactions involving iron (Hem, 1977). Molybdenum is considered to be an anionic species which is known to be immobilized by the adsorption or co-precipitation onto the active surface of ferric oxyhydroxides. Hem investigated the $\Delta G°$ values for two Mo oxides, MnO_3 and MnO_2, and a sulfide, MoS_2^-, as well as three dissolved Mo species; $H_2MoO_4(aq)$, $HMoO_4^-$, and MoO_4^{2-}. Thermodynamic data provide that $H_2MoO_4(aq)$ is dominant where pH<1.84 and MoO_4^{2-} is dominant where pH> 5.30. Eh-pH calculations for the oxides show that MoO_2 has a low solubility in reducing conditions where the pH is less than neutral, but MoO_2 is not known to exist as a natural mineral, therefore iron must be present as a possible control of Mo solubility which produces ferrous molybdate. At higher pH values the effect of the $FeOH^+$ complex is the principle cation whereas, at lower pH values the principle anion is $HMoO_4^-$ (Hem, 1977). Hem (1977) concluded that the theoretical chemical equilibrium models given in his study are useful in creating hypotheses for interpreting field data. Practical implications of hypotheses involving redox and precipitation processes at ferric hydroxide surfaces may facilitate prediction of trace metal behavior in aqueous environments, probable sites of and conditions leading to accumulation, and should aid in evaluating environmental effects (Hem, 1977).

Smedley and Edmunds (2002) investigated the redox patterns and the trace-metal behavior in the East Midlands Triassic Sandstone Aquifer of the United Kingdom. The purpose of their study was to examine the redox conditions that control the water chemistry. The study demonstrated that the complete reaction of oxygen is accompanied by a decrease in aquifer redox potential (Eh) of about 250 to 300 mV. The redox boundaries represent important geochemical interface controlling the speciation and, therefore, the mobility of many trace elements (i.e., As, Mo, Sb, Se, U, and Cr). They concluded that iron oxides play a key role in determining the spatial patterns in many of the trace metals studied as a result of Eh- and pH-controlled sorption/desorption reactions, as well as some reductive dissolution in the confined

portion of the aquifer. Groundwater pH was found to have an important control on the process of desorption of some metals, since the sorption of oxyanions onto iron oxides is known to be reduced at higher pH. Smedley and Edmunds (2002) describe Mo as having a distinct behavior from the other oxyanions as concentrations continue to increase uniformly down-gradient. The progressive increase in Mo down-gradient indicates that the element is not immobilized by the changing redox conditions.

Trace elements (e.g., Li, Rb, Sr, Mn, Mo and $\delta^{13}C$) have been used to derive a "chemical" timescale with which to determine age relationships in groundwaters for which no radiocarbon analyses are available (Edmunds and Smedley, 1998). Edmunds and Smedley (1998) objective is to investigate the possibility that time-dependent water-rock reactions may give rise to concentrations of trace elements present in the aquifer. A total of 45 samples were collected for the analysis of hydrogeochemical parameters as well as over 30 different trace metals (Edmunds and Smedley, 1998). In order to accomplish the objective the researchers plotted the concentrations of the trace elements as a function of temperature as an analogue of distance and/or depth.

Hydrogeochemical datum indicates that there is a well-defined redox boundary located in the aquifer ~4km from the recharge zone where oxygen has existed for several thousand years and there is a low facility for *in situ* reduction of contaminants (Edmunds and Smedley, 1998). Edmunds and Smedley chose Mo as a residence time indicator because it is unaffected by solubility controls, nor has it reached a plateau controlled by redox reactions or by partitioning between the solid and aqueous phases. To complete the study, Mo was plotted as a function of ^{14}C ages. Radiocarbon results display the groundwaters increasing in age along the west to east flow direction with ages in excess of 35 kyr BP (Edmunds and Smedley, 1998). Molybdenum was found to be unaffected by the redox reactions over the pH-Eh range in the aquifer. Edmunds and Smedley (1998) suggested that concentrations of Mo increase due to desorption of oxide surfaces, as a result of a reducing environment and microbial mediated

processes. Edmunds and Smedley (1998) concluded that the same chemical or isotopic indicators used in this study may be relevant to other groundwater studies provided that the lithology and mineralogy do not exhibit saturated concentrations of the indicator. In groundwater investigations a few radiocarbon analyses are important to obtain the relationship between concentration and age. Therefore the present approach offers a means of examining the residence time distribution more closely using chemical data and few radiocarbon analyses, offering a cost effective strategy for future groundwater studies (Edmunds and Smedley, 1998).

CHAPTER 7
CONCLUSION

The purpose of this research is to systematically examine and understand the biogeochemical mechanisms that control natural mobilization of Mo in the Aquia groundwater, Maryland, USA. The central hypothesis of this study was to determine the hydrogeochemical evolution along two separate groundwater flowpaths of the Aquia Aquifer, which consists of chemical weathering and oxidation/reduction reactions which are facilitated by the *in situ* microbial consortium (e.g., Fe reducers, SO_4^{2-} reducers), which catalyze both Mo mobilization, and capture by mineral/amorphous phases *via* adsorption/desorption reactions and/or mineral dissolution. To address this hypothesis, it was determined that this research would focus on the differences in groundwater evolution between the two Aquia Aquifer flowpaths with particular emphasis on describing Mo to interpret changing redox conditions.

Results indicate that Mo concentrations progressively increase along both flowpaths: the Eastern Shore Flowpath Mo concentrations increase from 0.011 to 0.354 μmol kg^{-1}, whereas the Western Shore Flowpath increases from 0.181 to 0.461 μmol kg^{-1}. Results also indicate that concentrations of Mo exhibit systematic changes along the flowpath that correspond to changes in Fe^{2+} and Fe^{3+} concentrations. Within the Eastern Shore flowpath Fe^{3+} is the dominant iron species until approximately 52 km down-gradient where Fe^{2+} becomes the more abundant form of iron (Figure 3). This change in iron species, as well as an increase in pH (>8.0), a decrease in Eh (-10.5 to -46 mV) and microbial mediated reduction, suggests that the reduction of Fe occurs at ~52km downgradient of the recharge area. With flow beyond 52 km, Fe^{3+} reduction is driven by Eh-pH relationship, ion-exchange reaction, and microbial dissimilatory processes which catalyze the release of Mo into solution (1.493 μmol kg^{-1}).

Further mobilization of Mo into the groundwater may be the result of newly formed minerals, as Fe^{3+} reduction proceeds, the released Fe^{2+} is likely the method of recrystallization of amorphous Fe^{3+} oxide/hydroxides into more thermodynamically stable and more crystalline Fe^{3+} oxides (Haque, 2008). However, at the end of the flowpath (>75 km) elevated Fe concentrations in conjunction with low Mo concentrations suggest that along this section of flow, Mo is being co-precipitated/re-adsorbed with more crystalline structures of these newly formed Fe sulfides (i.e., pyrite).

In the Western Shore flowpath the initiation of Fe^{3+} reduction is apparent at 42 km downgradient of the recharge area which coincides with the presence of cation-exchange reaction within the aquifer. At ~57 km the complete reduction of iron takes place making Fe^{2+} the dominant source of iron for the remainder of the flow. Flow beyond 57 km, reveals a progressive increase in Mo concentration (0.409 to 0.461 μmol kg^{-1}), indicating that the trace metal is not immobilized by changing redox conditions and can be associated with dissilimilatory Fe^{3+} reduction. An increase in HCO_3^- concentrations (>5.0 mmol kg^{-1}) at 57 km supports the evidence that bacterial reducing microbes such as, *Geobacter sp*. and *Shewenella putrifaciens* (Haque, 2008), utilize Fe^{3+} oxides as an electron acceptor to oxidize organic matter and result in an increase in Fe^{2+}. Sulfate reduction appears to occur at flow beyond 70 km. Sulfate-reducing bacteria have been observed in both flowpaths of the Aquia (Chapelle et al., 1987), and sulfate-reducing bacteria are expected to produce CO_2 from carbonaceous material, such as lignite (Knobel and Phillips, 1988; McMahon and Chapelle, 1991). Onset of more reducing conditions, at the end of the flowpath (>71 km), are distinguished by elevated Mo concentrations (0.461 μmol kg^{-1}) in conjunction with low Fe and S^{2-} concentrations which suggest that there is no co-precipitated/re-adsorption taking place, therefore, there is no evidence that pyrite is forming in the south-east end of the Western Shore flowpath.

Significant down-dip chemical changes in terms of redox conditions, pH, ion-exchange, and the concentration of a minor trace metal (Mo) are exhibited by groundwater in both

flowpaths. Mobility of Mo is directly affected by the activities of Fe and SO_4 reduction and/or reducing and oxidizing bacteria. The immobilization of Mo is most likely due to the adsorption onto oxy-hydroxides of Fe which is dependent on the Eh-pH relationship of the aqueous phase. A detailed analysis of porewater and sediment geochemistry is needed, in addition to groundwater sampling from wells to determine the effects of local microbial activity on groundwaters in the Aquia.

REFERENCES

Andreasen, D.C., 2002, Future of water supply from the Aquia and Magothy aquifers in southern Anne Arundel County, Maryland. *Maryland Department of Natural Resources Maryland Geological Survey*, www.mgs.md.gov.

Aeschbach-Hertig, W., Stute, M., Clark, J.F., Reuter, R.F., and Schlosser, P., 2002, A paleotemperature record derived from dissolved noble gases in groundwater of the Aquia Aquifer (Maryland, USA). *Geochimica et Cosmochimica Acta*, **66**(5), 797-817.

Algeo, T.J. and Lyons, T.W., 2006, Mo-total organic carbon covariation in modern anoxic marine environments: Implications for analysis of paleoredox and paleohydrographic conditions. Paleoceanography, 21, PA1016, doi:10.1029/2004PA001112.

Algeo, T.J., Lyons, T.W., Blakey, R.C., Over, J.D.,2007, Hydrographic conditions of the Devono-Carboniferous North American Seaway inferred from sedimentary Mo-TOC relationships. *Palaeogeography, Palaeoclimatology, Palaeoecology,* **256**, 204-230.

Algeo, T.J. and Maynard, J.B., 2008, Trace-metal covariation as a guide to water-mass conditions in ancient anoxic marine environments. *Geosphere*, **4**(5), 872-887.

Appelo, C.A.J., 1994, A Chromatographic Model for Water Quality Variations in the Aquia Aquifer (Maryland, USA). *Goldschmidt Conference Edinburgh*.

Appelo, C.A.J., 1994, Cation and Proton Exchange, pH variations, and Carbonate Reactions in a Freshening Aquifer. *Water Resource Research*, **30**(10), 2793-2805.

Bachman, L.J., Krantz, D.E., Böhlke, J., 2002, Hydrogeologic Framework, Ground-Water Geochemistry, and Assessment of Nitrogen Yield from Base Flow in Two Agricultural Watersheds, Kent County, Maryland. *U.S. Environmental Protection Agency, EPA/600/R-02/008*, 79 pg.

Barakso, J.J., Bradshaw, B.A., 1971, Molybdenum surface depletion and leaching. *Special volume – Canadian Institute of Mining and Metallurgy*, **11**, 78-84.

Bottrell, S.H., Moncaster, S.J., Tellam, J.H., Lloyd, J.W., Fisher, Q.J., Newton, R.J., 2000, Controls on bacterial sulphate reduction in a dual porosity aquifer system: the Lincolnshire Limestone aquifer, England. *Chemical Geology*, **169**, 461-470.

Brown, C.J., Schoonen, M.A.A., Candela, J.L., 2000, Geochemical modeling of iron, sulfur, oxygen and carbon in a coastal plain aquifer. *Journal of Hydrology*, **237**, 147-168.

Champ, D.R., Gulens, J., Jackson, R.E., 1979, Oxidation-reduction sequences in groundwater flow systems. *Canadian Journal Earth Science*, **16**, 12-23.

Chapelle, F.H., 1983, Groundwater Geochemistry and Calcite Cementation of the Aquia Aquifer in Southern Maryland. *Water Resource Research*, **19**, 545-558.

Chapelle, F.H., Knobel, L.L., 1983, Aqueous Geochemistry and the Exchangeable Cation Composition of Gluaconite in the Aquia Aquifer, Maryland. *Ground Water*, **21**(3), 343-352.

Chapelle, F.H., Knobel, L.L., 1985, Stable Carbon Isotopes of HCO^-_3 in the Aquia Aquifer, Maryland: Evidence for an Isotopically Heavy Source of CO_2. *Groundwater,* **23**, 592-599.

Chapelle, F.H., Bradley, P.M., 1998, Selecting Remediation Goals by Assessing the Natural Attenuation Capacity of Groundwater Systems. *U.S. Geological Survey, Columbia,SC*, 227-238.

Chapelle, F.H., 2001, Ground-Water Microbiology and Geochemistry. New York: *John Wiley & Sons, Inc*., 424p.

Crusius, J., Calvert, S., Pedersen, T., Sage, D., 1996, Rhenium and molybdenum enrichments in sediments as indicators of oxic, suboxic and sulfidic conditions of deposition. *Earth and Planetary Science Letters*, **145**, 65-78.

Crusius, J., Thomson, J., 2000, Comparative behavior of authigenic Re, U, and Mo during reoxidation and subsequent long-term burial in marine sediments. *Geochimica et Cosmochimica Acta*, **64**(13), 2233-2242.

Dai, Z., Samper, J., 2006, Inverse modeling of water flow and multicomponent reactive transport in coastal aquifer systems. *Journal of Hydrology*, **327**, 447-461.

Dai, Z., Samper, J., Ritzi Jr., R., 2006, Identifying geochemical processes by inverse modeling of multicomponent reactive transport in the Aquia Aquifer. *Geoshere*, **2**(4), 210-219.

Dalai, T.K., Nishimura, K., Nozaki, Y., 2005, Geochemistry of molybdenum in the Chao Phraya River estuary, Thailand: Role of suboxic diagenesis and porewater transport. *Chemical Geology*, **218**, 189-202.

Edmunds, W.M., Bath, A.H., Miles, D.L., 1982, Hydrochemical evolution of the East Midlands Triassic sandstone aquifer, England. *Geochimica et Cosmochimica Acta*, **46**, 2069-2081.

Edmunds, W.M. and Walton, N.R.G., 1983, The Lincolnshire Limestone – Hydrogeochemical Evolution Over a Ten-Year Period. *Journal of Hydrology*, **61**, 201-211.

Edmunds, W.M. and Smedley, P.L., 1998, Trace elements as residence time indicators in groundwaters; the East Midlands Triassic sandstone aquifer, England. *International Symposium on Water-Rock Interaction*, **9**, 215-218.

Edmunds, W.M., Carrillo-Rivera, J.J., Cardona, A., 2002, Geochemical evolution of groundwater beneath Mexico City. *Journal of Hydrology*, **258**, 1-24.

Erickson, B.E., Helz, G.R., 2000, Molybdenum(VI) speciation in sulfidic waters: Stability and lability of thiomolybdates. *Geochimica et Cosmochimica Acta*, **64**(7), 1149-1158.

Frank, A., 1998, 'Mysterious' moose disease in Sweden. Similarities to copper deficiency and/or molybdenosis in cattle and sheep. Biochemical background of clinical signs and organ lesions. *The Science of the Total Environment*, **209**, 17-26.

Groffman, A.R., Crossey, L.J., 1999, Transient redox regimes in a shallow alluvial aquifer. *Chemical Geology*, **161**, 415-442.

Gustafsson, J.P., 2003, modeling molybdate and tungstate adsorption to ferrihydrite. *Chemical Geology*, **200**, 105-115.

HACH, 2009. HACH DR/890 Colorimeter Procedures Manual. USA.

Haque, S.E., 2007, Hydrogeochemical evolution of arsenic along groundwater flowpaths: Linking aqueous and solid phase arsenic speciation: University of Texas at Arlington, PhD Thesis.

Haque, S.E., Ji, J., Johannesson, K.H., 2008, Evaluating mobilization and transport of arsenic in sediments and groundwaters of Aquia Aquifer, Maryland, USA. *Journal of Contaminant Hydrology*, doi: 10.1016/j.jconhyd.2008.03.003.

He, Z.L., Yang, X.E., Stoffella, P.J., 2005, Trace elements in agroecosystems and impacts on the environment. *Journal of Trace Elements in Medicine and Biology*, **19**, 125-140.

Hearne, G.A., and Litke, D.W., 1987, Ground-water flow and quality near Canon City, Colorado. *U.S. Geological Survey, Water-Resources Investigations Report 87-4014*, 71.

Helz, G.R., Miller, C.V., Charnock, J.M., Mosselmans, J.F.W., Pattrick, R.A.D., Garner, C.D., and Vaughan, D.J., 1996, Mechanism of molybdenum removal from the sea and its concentration in black shales: EXAFS evidence. *Geochimica et Cosmochimica Acta*, **60**(19), 3631-3642.

Hem, J.D., 1977, Reactions of metal ions at surfaces of hydrous iron oxide. *Geochimica et Cosmochimica Acta*, **41**, 527-538.

Hodge, V.F., Johannesson, K.H., Stetzenbach, K.J., 1996, Rhenium, molybdenum, and uranium in groundwater from the southern Great Basin, USA: Evidence for conservative behavior. *Geochimica et Cosmochimica Acta*, **60**(17), 3197-3214.

Hunter, K.S., Wang, Y., Van Cappellen, P., 1998, Kinetic modeling of microbially-driven redox chemistry of subsurface environments: coupling transport, microbial metabolism and geochemistry. *Journal of Hydrology*, **209**, 53-80.

Jakobsen, R., and Postma, D., 1999, Redox zoning, rates of sulfate reduction and interactions with Fe-reduction and methanogenesis in a shallow sandy aquifer, Romo, Denmark, *Geochimica et Cosmochimica Acta*, **63**, 137-151.

Johannesson, K.H., Lyons, W.B., Graham, E.Y., Welch, K.A., 2000, Oxyanion concentrations in Eastern Sierra Nevada rivers - 3. Boron, Molybdenum, Vanadium, and Tungsten. *Aquatic Geochemistry*, **6**, 19-46.

Kaback, D.S., Runnells, D.D., 1979, Geochemistry of molybdenum in some stream sediments and waters. *Geochimica et Cosmochimica Acta*, **44**, 447-456.

Kehew, A.E., 2001, Applied Chemical Hydrogeology. *New Jersey: Prentice Hall*, 368 p.

Klohe, C.A., Kay, R.T., 2007, Hydrogeology of the Piney Point-Nanjemoy, Aquia, and Upper Patapsco aquifers, Naval Air Station Patuxent River and Webster Outlying Field, St. Mary's County, Maryland, 2000-6. *Geological Survey Scientific Investigations Report 2006-5266*, 26p.

Knobel, L.L., Chapelle, F.H., Phillips, S.W., 1987, Overview of geochemical processes controlling the chemistry of water in the Aquia and Magothy aquifers, northern Atlantic Coastal Plain. *American Water Resources Association*, **9**, 25-37.

Lovley, D.R., and Chapelle, F.H., 1995, Deep subsurface microbial processes, *Rev. Geophysics*, **33**, 365-381.

Lovley, D.R., 1997, Microbial Fe(III) reduction in subsurface environments, *FEMS Microbiology Reviews*, **20**, 305-313.

Leybourne, M.I., and Cameron, E.M., 2007, Source, transport, and fate of rhenium, selenium, molybdenum, arsenic, and copper in groundwater associated with porphyry-Cu deposits, Atacama Desert, Chile. *Chemical Geology* doi:10.1016/j.chemgeo.2007.10.017.

Magyar, B., Moor, H.C., Sigg, L., 1993, Vertical distribution and transport of molybdenum in a lake with a seasonally anoxic hypolimnion. *Limnol. Oceanogr.,* **38(3)**, 521-531.

McBride, M.B., 1994, Environmental Chemistry of Soils. *New York: Oxford University Press*, 406p.

McEwan, A.G., Ridge, J.P., McDevitt, C.A., 2001, The DMSO reductase family of microbial molybdenum enzymes; molecular properties and role in the Dissimilatory reduction of toxic elements. *Geomicrobiology Journal*, **19**, 3-21.

Moncaster, S.J., Bottrell, S.H., Tellam, J.H., Lloyd, J.W., Konhauser, K.O., 2000, Migration and attenuation of agrochemical pollutants: insights from isotopic analysis of groundwater sulphate. *Journal of Contaminant Hydrology*, **43**, 147-163.

Morgan-Jones, M., Eggboro, M.D., 1981, The hydrogeochemistry of the Jurassic limestone in Gloucestershire, England. *Q.J. eng. Geol. London*, **14**, 25-39.

Morgan-Jones, M., 1985, The hydrogeochemistry of the Lower Greensand aquifers south of London, England. *Q.J. eng. Geol. London*, **18**, 443-458.

Nealson, K.H. and Myers, C.R., 1992, Microbial Reduction of Manganese and Iron: New Approaches to Carbon Cycling. *Applied and Environmental Microbiology*, 439-443.

Penny, E., and Lee, M., 2003, Groundwater and microbial processes of Alabama coastal plain aquifers. *Water Resources Research*, **39**(11), 1320-1337.

Postma, D., Jakobsen, R., 1996, Redox zonation: Equilibrium constraints on the $Fe3+/SO_4$-reduction interface. *Geochimica et Cosmochimica Acta*, **60**(17), 3169-3175.

Purdy, C.B., Mignerey, A.C., Helz, G.R., 1987, ^{36}Cl: A Tracer in Groundwater in the Aquia Formation of Southern Maryland. *Nuclear Instruments and Methods in Physics Research*, **B29**, 372-375.

Purdy, C.B., Burr, G.S., Rubin M., Helz, G.R., Mignerey, A.C., 1991, Dissolved organic and inorganic ^{14}C concentrations and ages for coastal plain aquifers in southern Maryland. *Radiocarbon*, **34**(3), 654-663.

Purdy, C.B., Burr, G.S., Rubin, M., Helz, G.R., Mignerey, A.C., 1992, Dissolved Organic and Inorganic ^{14}C Concentrations and Ages for Coastal Plain Aquifers in Southern Maryland. *Radiocarbon*, **34**(3), 654-663.

Purdy, C.B., Helz, G.R., Mignerey, A.C., 1996, Aquia Aquifer Dissolved Cl^- and $^{26}Cl/Cl$: Implications for Flow velocities. *Water Resources Research*, **32**(5), 1163-1171.

Reynolds, B.C., Wasserburg, G.J., Baskaran, M., 2003, The transport of U- and Th-series nuclides in sandy confined aquifers. *Geochimica et Cosmochimica Acta*, **67**(11), 1955-1972.

Schlieker, M., Schüring, J., Hencke, J., Schulz, H.D., 2001, The influence of redox processes on trace element mobility in a sandy aquifer—an experimental approach. *Journal of Geochemical Exploration*, **73**, 167-179.

Schürch, M., Edmunds, W.M., Buckley, D., 2004, Three-dimensional flow and trace metal mobility in shallow Chalk groundwater, Dorset, United Kingdom. *Journal of Hydrology*, **292**, 229-248.

Smedley, P.L., Edmunds, W.M., 2002, Redox Patterns and Trace-Element behavior in the East Midlands Triassic Sandstone Aquifer, U.K. *Ground Water*, **40**(1), 44-58.

Sohrin, Y., Matsui, M., Nakayama,E., 1999, Contrasting behavior of tungsten and molybdenum in the Okinawa Trough, the East China Sea and the Yellow Sea. *Geochimica et Cosmochimica Acta*, **63**(19/20), 3457-3466.

Tribovillard, N., Algeo, T.J., Lyons, T., Riboulleau, A., 2006, Trace metals as paleoredox and paleoproductivity proxies: An update. *Chemical Geology*, **232**, 12-32.

Tribovillard, N., Bout-Roumazeilles, V., Algeo, T., Lyons, T.W., Sionneau, T., Montero-Serrano, J.C., Riboulleau, A., Baudin, F., 2008, Paleodepositional condition n the Orca Basin as inferred from organic matter and trace metal contents. *Marine Geology,* **254**, 62-72.

Vanbroekhoven, K., Van Roy, S., Geilen, C., Maesen, M., Ryngaert, A., Diels, L., Seuntjens, P., 2007, Microbial processes as key drivers for metal (im)mobilization along a redox gradient in the saturated zone. *Environmental Pollution* **148**, 759-769.

Vartak, S.V., 1996, Separation studies of molybdenum (VI) and rhenium (VII) using TPPO as an extractant. *Talanta*, **43**, 1465-1470.

Vengosh, A., Hening, S., Ganor, J., Mayer, B., Weyhenmeyer, C.E., Bullen, T.D., Payton, A., 2007, New isotopic evidence for the origin of groundwater from the Nubian Sandstone Aquifer in the Negev, Israel. *Applied Geochemistry* **22**, 1052-1073.

Vorlicek, T.P., and Helz, G.R., 2002, Catalysis by mineral surfaces: Implications for Mo geochemistry in anoxic environments. *Geochimica et Cosmochimica Acta*, **66**(21), 3679-3692.

Vorlicek, T.P., Kahn, M.D., Kasuya, Y., Helz, G.R., 2004, Capture of molybdenum in pyrite-forming sediments: Role of ligand-induced reduction of polysulfides. *Geochimica et Cosmochimica Acta,* **68**(3), 547-556.

BIOGRAPHICAL INFORMATION

Teresa Marie Iafelice Valle was born to Donald and Kimberly Iafelice, on July 6, 1977, in the British Royal Hospital at York Barracks, Muenster, West Falia, Germany. During the years 1977 through 1980, Teresa's father was serving in the U.S. Army as a Sergeant attached to the British Royal Army as a Communication Specialist during the Cold War. After graduating from high school in Tyler, Texas, and marrying her high-school sweetheart, Teresa began her journey to obtain a college degree in the spring of 2002. While taking Physical and Historical Geology, Teresa realized that she enjoyed the subject and continued studying Geology.

In December 2006, Teresa received her Bachelor of Science in Geology with the honor Cum Laude from the University of Texas at Arlington. While working toward her Masters degree in Geology at the University of Texas at Arlington, focusing on the geochemical changes of molybdenum in groundwaters, Teresa was employed at the University as a graduate teaching assistant, instructing the labs for Historical and Physical Geology. Upon completion of her Masters in December 2009, Teresa plans on pursuing her interests in the Oil and Gas Industry.